Diastereoselective and Reversible Metallacycle Formation by Attack of a Pt-PR_2OH Group on a Coordinated Nitrile in Pt-Catalyzed Hydration

Jorge A. Garduño,[a] Andrew J. Sasser,[a] Hannah J. Sexton,[a] Russell P. Hughes,[a] David S. Glueck,[a]* and Arnold L. Rheingold[b]

[a] 6128 Burke Laboratory, Department of Chemistry, Dartmouth College, Hanover, New Hampshire 03755, United States [b] Department of Chemistry, University of California, San Diego, 9500 Gilman Dr., La Jolla, California 92093, United States

ABSTRACT: Kinetic resolution of the racemic nitrile CH(Et)(CN)(*cyclo*-$N(CH_2)_3C(O)$-) by catalytic asymmetric hydration to form the amide CH(Et)($C(O)NH_2$)(*cyclo*-$N(CH_2)_3C(O)$-) (Levetiracetam, Keppra) is an industrial biocatalytic process. To develop analogous procedures using chiral metal complexes as catalyst precursors, we investigated the mechanism and selectivity of the individual steps. Treatment of Pt(diphos)Cl_2 with AgOTf and secondary phosphine oxides (SPOs) gave the cations [Pt(diphos)(PR'_2OH)(Cl)][OTf] **1-6** containing either a chiral diphos ((*R,R*)-FerroLANE derivatives or (*S,S*)-Et-FerroTANE) or a chiral SPO tautomer ((*R*)-DMB-SPOPine). A second equiv of AgOTf yielded dicationic [Pt(diphos)(PR'_2OH)][$OTf]_2$ (**9-12** and **14**), with Fe-Pt interactions, or [Pt((*S,S*)-Et-FerroTANE)(PMe_2OH)(OTf)][OTf] (**13**). Pt complexes **9** and **11-14** catalyzed hydration of the Keppra nitrile to the amide under mild conditions, with increased activity for smaller FerroLANE substituents. With water as the limiting reagent and an excess of racemic nitrile, no enantioselectivity in kinetic resolution by catalytic nitrile hydration was observed. Reaction of [Pt(*R,R*)-Me-FerroLANE)(PMe_2OH)][$OTf]_2$ (**9**) with enantiomerically enriched or racemic Keppra nitrile resulted in diastereoselective and reversible metallacycle formation to give [Pt((*R,R*)-Me-FerroLANE)($PMe_2OC(R^*)$=NH][$OTf]_2$ (**15**, R* = CH(Et)(*cyclo*-$N(CH_2)_3C(O)$-)). Similar processes occurred with dications **10-11** and **13-14** with *rac*-Keppra nitrile, or with **9** and *rac*-PhCH(R)(CN) (R = Me, Et, *i*-Pr, Cy) or with racemic *cyclo*-Ph_2CCH_2CH(CN) to generate metallacycles **16-24**. Metallacycle **15** reacted with water by attack at the PMe_2O group, demonstrated by ^{18}O-labeling studies, to yield the Keppra amide via an intermediate iminol complex [Pt((*R,R*)-Me-FerroLANE)(PMe_2OH)(NH=C(R^*)(OH))][$OTf]_2$ (**25**).

INTRODUCTION

Synthesis of amides by hydration of nitriles is an atom economical approach to an important functional group.[1] Catalytic methods are valuable to avoid undesired formation of carboxylic acids and increase the selectivity,[2] and biocatalytic processes with the enzyme nitrile hydratase[3] have been commercialized.[4] Even higher selectivity was required in another industrial process for synthesis of the blockbuster anti-epilepsy drug Levetiracetam (Keppra), in which an engineered enzyme catalyzed kinetic resolution of a racemic nitrile to yield an enantioenriched *S*-amide (Scheme 1).[5] Base-mediated racemization of the recovered *R*-nitrile enabled recycling and a higher overall yield. In contrast, related kinetic resolutions of racemic nitriles by abiological catalytic asymmetric nitrile hydration are extremely rare and have limited substrate scope and enantioselectivity.[6] The potential value of such processes was highlighted by their inclusion on the American Chemical Society Green Chemistry Institute Pharmaceutical Roundtable's 2007 list of "aspirational reactions" for future development.[7]

Scheme 1. Application of enzyme-catalyzed kinetic resolution via nitrile hydration to synthesis of Levetiracetam (Keppra)

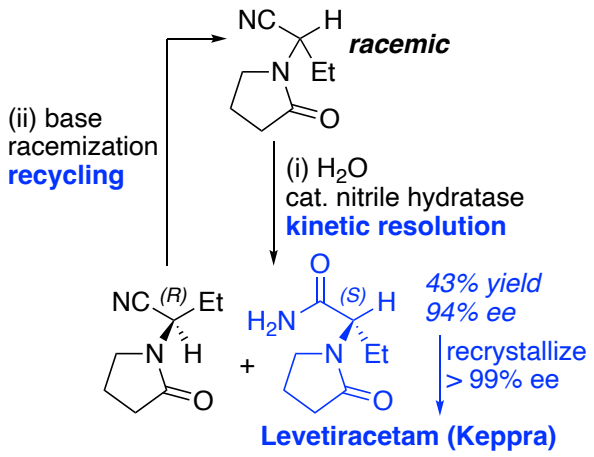

To develop chiral metal complexes as catalyst precursors for kinetic resolution of racemic nitriles, we considered the proposed mechanism of a popular class of Pt catalysts bearing PMe_2OH (phosphinous acid) ligands,[8] formed by tautomerization of secondary phosphine oxide (SPO) precursors (Scheme 2).[9] As first proposed

by Ghaffar and Parkins,[10] and recently observed directly, the key step is nucleophilic attack of the pendant PMe_2OH oxygen on coordinated nitrile to yield a metallacycle.[11] After attack of water at phosphorus and a series of proton transfers, the catalyst forms the amide and rebinds a nitrile for the next cycle. With a chiral catalyst, several individual steps might contribute to the desired enantioselectivity. Scheme 2 shows a proposed catalytic cycle for kinetic resolution of a racemic nitrile, in which the blue *R* enantiomer reacts more quickly than the black *S* one. Selective coordination of one nitrile enantiomer to Pt could yield a mixture of diastereomers $\mathbf{A_R}$ and $\mathbf{A_S}$, under kinetic or thermodynamic control.[12] Similarly, one of the metallacycles ($\mathbf{B_R}$ or $\mathbf{B_S}$) might form more quickly than the other (rate constants k_R and k_S), or be preferred thermodynamically, if both nitrile coordination and metallacycle formation were reversible. Finally, if one metallacycle reacted faster than the other with water ($k'_R > k'_S$), this irreversible step could result in selective amide formation.

To investigate these ideas, we report here the synthesis of a series of chiral catalyst precursors $[Pt(diphos^*)(PR_2OH)]^{2+}$, their use in nitrile hydration, and direct observation of both diastereoselective, reversible, metallacycle formation and reaction with water to yield amide products and regenerate the catalyst. The resulting structure-property-activity relationships are potentially valuable in design and development of more active and selective catalysts.

Scheme 2. Proposed mechanism of kinetic resolution of a racemic nitrile (R*CN = CHR'(R'')(CN)) via hydration catalyzed by a chiral $[Pt(diphos^*)(PR_2OH)]^{2+}$ dication ([Pt] = Pt(diphos*)), with selectivity controlled in nitrile coordination, metallacycle formation, and water attack steps

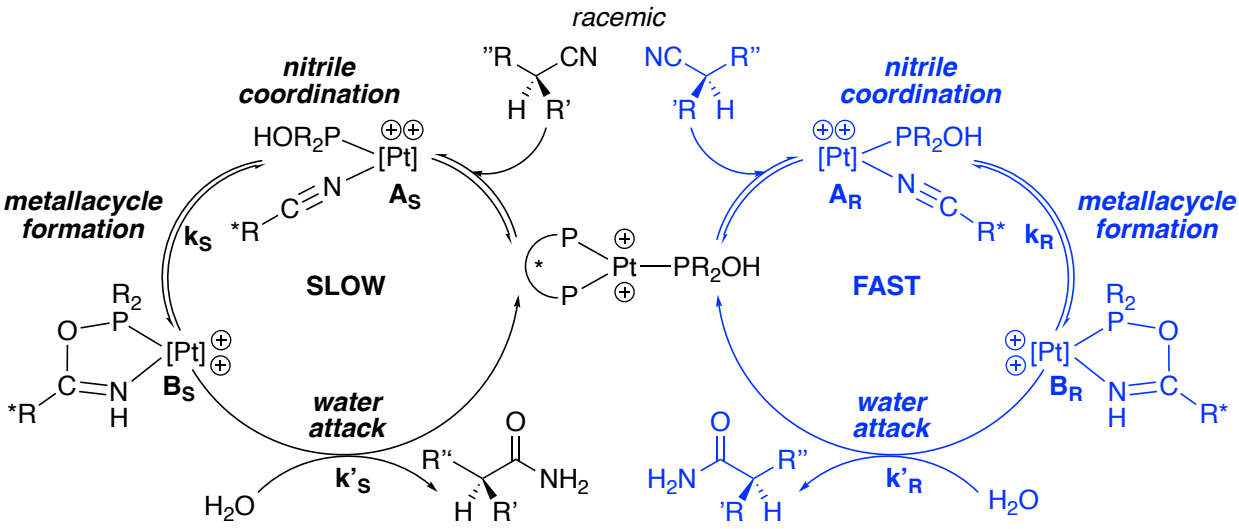

RESULTS AND DISCUSSION

Synthesis and Structure of Catalyst Precursors To prepare chiral analogues of the bis(phosphino)ferrocene-ligated catalyst precursor $[Pt(dppf)(PMe_2OH)(Cl)][OTf]$,[11] we selected the commercially available (*R,R*)-FerroLANE and (*S,S*)-Et-FerroTANE ligands to systematically vary their size by changing the P-donor substituents.[13] Alternatively, we replaced PMe_2OH in the dppf precursor with the chiral binaphthyl-based phosphepine SPO tautomer (*R*)-DMB-SPOPine (DMB = dimethylbinaphthyl; see **14** in Scheme 3 below for the structure).[6]

Chloride abstraction from $Pt(diphos^*)Cl_2$ (diphos* = (*R,R*)-Me-FerroLANE, (*R,R*)-Et-FerroLANE, or (*S,S*)-Et-FerroTANE)[14] with AgOTf in the presence of $PMe_2(O)H$ gave cationic complexes **1**-**2** and **5**-**6** (Scheme 3).[15] This approach was less successful for bulkier SPOs and diphos* ligands. For example, with (*R,R*)-*i*-Pr-FerroLANE, tautomerization/P-coordination of $PMe_2(O)H$ was slow, and SPO O-coordination in $[Pt((R,R)\text{-}i\text{-Pr-FerroLANE})(OPMe_2(H))(Cl)][OTf]$ was observed by $^{31}P\{^1H\}$ NMR spectroscopy. Instead, treatment of $Pt((R,R)\text{-Me-FerroLANE})Cl_2$ with AgOTf and the chlorophosphines PR_2Cl generated the cations $[Pt((R,R)\text{-Me-FerroLANE})(PEt_2Cl)(Cl)][OTf]$ (**7**) and $[Pt((R,R)\text{-}i\text{-Pr-FerroLANE})(PMe_2Cl)(Cl)][OTf]$ (**8**). P–Cl hydrolysis followed by addition of AgOTf generated **3**-**4** (Scheme 3).[16] The phosphinous acid complexes had characteristic $^{31}P\{^1H\}$ spectra (Table 1), with large trans J_{PP} coupling constants (ca. 400 Hz), and broad P-OH ^1H NMR signals around 9-10 ppm in CD_2Cl_2.

Treatment of Pt-Cl cations **1**-**4** and **5** with AgOTf gave "three-coordinate" dications **9**-**12** and **14** (Scheme 3), for which the A_2X doublet/triplet patterns in the $^{31}P\{^1H\}$ NMR spectra were consistent with Fe→Pt dative interactions, as observed in related complexes.[17,11,15] Despite the structural similarity of Et-FerroTANE to Me-FerroLANE and dppf ligands, the $^{31}P\{^1H\}$ NMR spectrum of **13**, formed from **6** and AgOTf, showed that it was four-coordinate, with inequivalent FerroTANE ^{31}P nuclei and, presumably, a coordinated triflate.

The crystal structure of PEt_2OH complex **2** (Figure 1) was similar to that of the PMe_2OH complex **1** and several related derivatives with different diphos ligands,[11,15] with a large Me-FerroLANE bite angle of 100.78(7)°.[18]

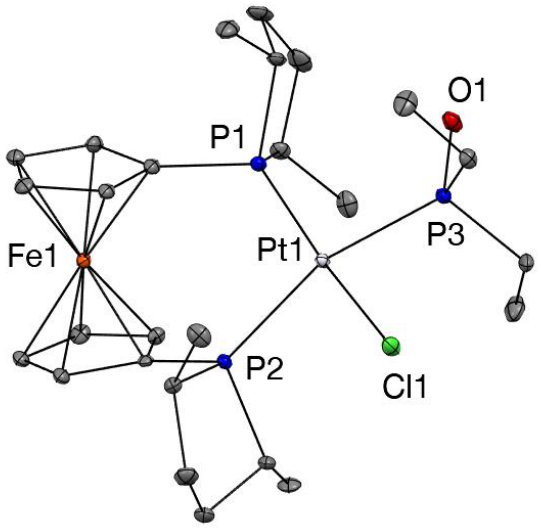

Figure 1. ORTEP diagram of the cation in [Pt(*R,R*)-Me-FerroLANE)(PEt$_2$OH)(Cl)][OTf] (**2**)

Scheme 3. Synthesis of [Pt(diphos)(PR'$_2$OH)(Cl)][OTf] cations **1-6** and their conversion to the dications [Pt(diphos)(PR'$_2$OH)][OTf]$_2$ **9-12** and the cation **13** (diphos = (*R,R*)-FerroLANE (**1-4**, **7-11**), (*S,S*)-Et-FerroTANE) (**5** and **13**), or dppf (**6** and **14**). For the FerroLANE complexes, R' = Me; R = Me (**1** and **9**), Et (**2** and **10**), *i*-Pr (**3**, **8** and **11**); R' = Et, R = Me (**4**, **7** and **12**)

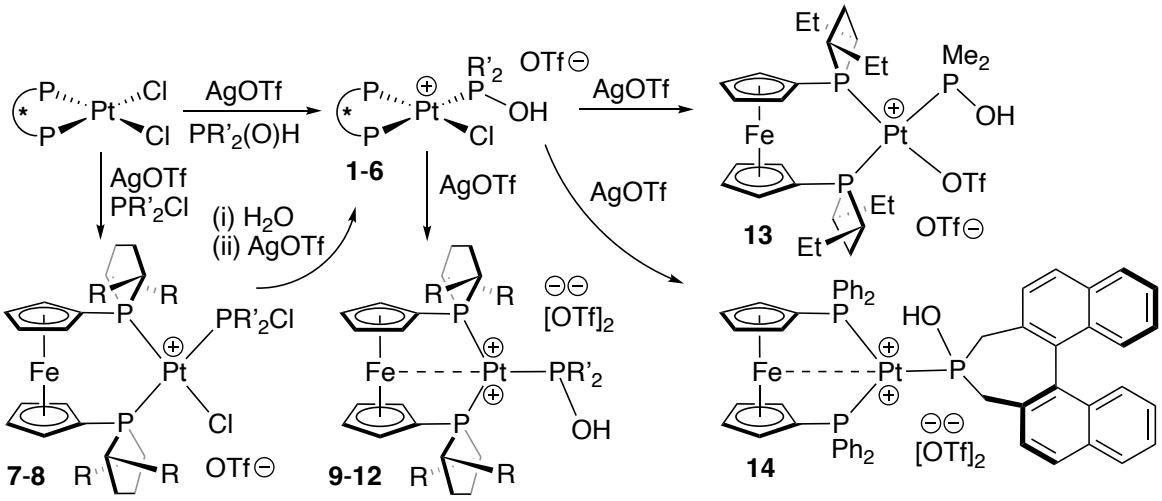

Table 1. $^{31}P\{^{1}H\}$ NMR Data for the Complexes [Pt(diphos*)(PR'$_2$OH)(Cl)][OTf] (**1-6**), [Pt(diphos*)(PR'$_2$OH)][OTf]$_2$ (**9-12** and **14**), [Pt(*S,S*)-Et-FerroTANE)(PMe$_2$OH)(OTf)][OTf] (**13**), metallacycles [Pt(diphos*)(PR'$_2$OC(R*)=NH)][OTf]$_2$ (**15-24**), iminol complexes [Pt((*R,R*)-Me-FerroLANE)(PMe$_2$OH)(NH=C(R*)(OH))][OTf]$_2$ **25**, and aquo adduct [Pt(*R,R*)-Me-FerroLANE)(PMe$_2$OH)(OH$_2$)][OTf]$_2$ (**26**) [a]

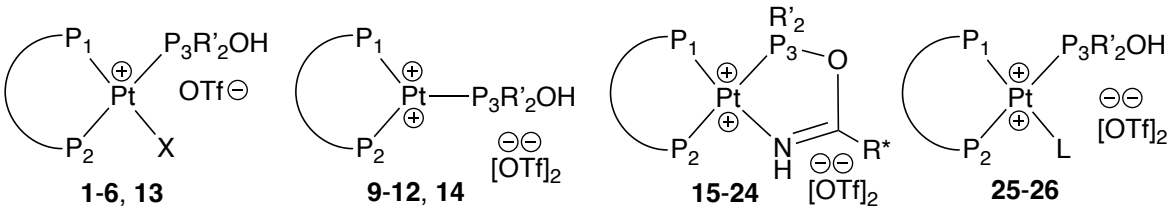

No.	diphos* (dr)	R'	X	δ(^{31}P$_1$) (J_{Pt-P})	δ(^{31}P$_2$) (J_{Pt-P})	δ(^{31}P$_3$) (J_{Pt-P})	J_{12}	J_{13}	J_{23}
1	(*R,R*)-Me-FerroLANE	Me	Cl	37.6 (3617)	36.9 (2142)	96.7 (2784)	12	27	458
2	(*R,R*)-Me-FerroLANE	Et	Cl	37.8 (3646)	37.9 (2148)	113.1 (2799)	12	24	438
3	(*R,R*)-Et-FerroLANE	Me	Cl	32.4 (3623)	34.2 (2156)	95.8 (2794)	11	26	458
4	(*R,R*)-*i*-Pr-FerroLANE	Me	Cl	19.8 (3613)	29.2 (2147)	91.5 (2821)	10	28	456
5	(*S,S*)-Et-FerroTANE	Me	Cl	36.7 (3374)	40.5 (1973)	94.8 (2813)	nd	nd	438
13	(*S,S*)-Et-FerroTANE	Me	OTf	40.0 (3876)	53.2 (2030)	99.8 (2886)	nd	31	379
6	dppf	*R*-DMB	Cl	12.5 (3820)	20.7 (2160)	106.0 (2678)	16	21	436
9	(*R,R*)-Me-FerroLANE	Me	--	18.9 (2236)		86.9 (4473)		13	
10	(*R,R*)-Me-FerroLANE	Et	--	18.8 (2227)		112.3 (4454)		11	
11	(*R,R*)-Et-FerroLANE	Me	--	7.3 (2194)		87.9 (4544)		12	
12	(*R,R*)-*i*-Pr-FerroLANE	Me	--	–6.0 (2179)		87.1 (4695)		12	
14	dppf	*R*-DMB	--	–12.3 (2448)		105.7 (4046)		12	
***S*-15**	(*R,R*)-Me-FerroLANE	Me	*S*-PMe$_2$OC(R*)=NH	25.0 (3159)	37.8 (2435)	164.9 (2412)	13	21	355
***R*-15**	(*R,R*)-Me-FerroLANE	Me	*R*-PMe$_2$OC(R*)=NH	24.8 (3144)	38.3 (2442)	163.6 (2422)	14	21	355
16	(*R,R*)-Me-FerroLANE dr = 1.6	Et	PMe$_2$OC(R*)=NH	25.0 (3142) 24.7 (3123)	37.2 (2425) 37.8 (2437)	181.5 (2385) 180.2 (2386)	13 14	19 19	334 336
17	(*R,R*)-Et-FerroLANE dr = 1.7	Me	PMe$_2$OC(R*)=NH	22.3–21.8 (3142)	34.9 (2430) 35.2 (2435)	164.1 (2403) 162.9 (2411)	13 13	20 21	353 353
18	(*S,S*)-Et-FerroTANE dr = 1.2	Me	PMe$_2$OC(R*)=NH	27.3 (2933) 25.1 (2999)	45.7 (2328) 43.8 (2333)	163.8 (2408) 163.6 (2406)	15 nd	20 20	338 338
19	Dppf dr = 1.1	*R*-DMB	PMe$_2$OC(R*)=NH	0.5-0.0 (3378)	19.3 (2695)	187.8 (2394) 188.1 (2402)	13 13	16 16	354 353
20	(*R,R*)-Me-FerroLANE dr = 1	Me	PMe$_2$OC(R*)=NH R* = PhCH(Me)	26.4-25.9 (3183)	36.5 (2418) 36.3 (2432)	162.8 (2440) 162.6 (2440)	13 13	21 21	360 360
21	(*R,R*)-	Me	PMe$_2$OC(R*)=NH	25.7 (3166)	37.1 (2447)	162.6 (2411)	13	21	357

	Me-FerroLANE dr = 1.1		R* = PhCH(Et)	25.9 (3164)	36.9 (2447)	162.5 (2411)	14	20	357
22	(*R*,*R*)- Me-FerroLANE dr = 1.2	Me	$PMe_2OC(R^*)$=NH R* = PhCH(*i*-Pr)	24.9 (3103) 24.0 (3096)	38.6 (2401) 39.8 (2411)	162.6 (2355) 162.4 (2355)	13 13	21 21	349 347
23	(*R*,*R*)- Me-FerroLANE dr = 1.3	Me	$PMe_2OC(R^*)$=NH R* = PhCH(Cy)	24.8 (3098) 23.9 (3098)	38.7 (2408) 39.8 (2411)	162.4 (2357) 162.1 (2359)	13 13	21 21	348 346
24	(*R*,*R*)- Me-FerroLANE dr = 1.6	Me	$PMe_2OC(R^*)$=NH $R^* = Ph_2CCH_2CH$	23.3 (3084) 24.1 (3075)	40.8 (2420) 37.9 (2398)	156.9 (2346) 157.5 (2350)	15 15	22 20	346 345
***S*-25**	(*R*,*R*)- Me-FerroLANE	Me	*S*-NH=C(R*)(OH)	22.4 (3191)	35.4 (2123)	87.2 (2849)	nd	29	413
***R*-25**	(*R*,*R*)- Me-FerroLANE	Me	*R*-NH=C(R*)(OH)	22.6 (3149)	34.3 (2143)	88.2 (2844)	14	31	412
26	(*R*,*R*)- Me-FerroLANE	Me	H_2O	32.8 (3933)	46.2 (2150)	97.2 (2781)	nd	25	418

[a] Minor isomer listed first for diastereomers. For metallacycles **15-19** and iminol complexes **25**, R* is derived from the Keppra nitrile. Not determined = nd. Solvent = CH_2Cl_2 or CD_2Cl_2, $^{31}P\{^1H\}$ NMR chemical shift reference = 85% H_3PO_4.

Structure-Activity Relationships in Pt-Catalyzed Nitrile Hydration We chose the Keppra nitrile (Scheme 1) as a model hydration substrate because highly enantiomerically enriched material can be prepared in one step from the commercially available amide drug,[19] and base-mediated epimerization gives the racemic nitrile.[5b] Kinetic resolution by Pt-catalyzed nitrile hydration was investigated using water as the limiting reagent at room temperature (Scheme 4 and Tables S1-S2 in the Supporting Information). Catalytic turnover frequency depended strongly on the size of the diphos* and SPO ligands. Under comparable kinetic resolution conditions with 1 mol % loading, hydration of racemic Keppra-nitrile with 0.2 equiv of water by Me-FerroLANE catalyst precursor **9** was complete after 15 min, while *i*-Pr-FerroLANE precursor **12** promoted only 15% conversion even after 7 d. Et-FerroTANE catalyst precursor **13** had activity comparable to that of **9**, while switching from PMe_2OH in **9** to PEt_2OH in **12** reduced the rate approximately two-fold. Disappointingly, no enantioselectivity was observed with any of the catalyst precursors. A control experiment showed that enantiopure nitrile was converted to enantiopure amide using precursor **9** and one equiv of water, ruling out epimerization of the product under the reaction conditions. Hydration of the Keppra nitrile with precursor **9** was significantly faster for H_2O than D_2O, with approximately three times more conversion after 15 min.

Scheme 4. Attempted kinetic resolution of racemic Keppra-nitrile by Pt-catalyzed hydration

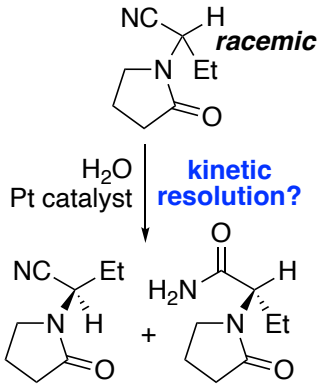

Mechanistic Studies. 1. Reversible Metallacycle Formation with Thermodynamic Diastereoselectivity To study the mechanism of the catalytic reactions and to rationalize their lack of stereoselectivity, we investigated the individual steps in the proposed catalytic cycle (Scheme 2). Treatment of [Pt((*R*,*R*)-Me-FerroLANE)(PMe_2OH)][OTf]$_2$ (**9**) with 3 equiv of (*S*)-Keppra nitrile gave metallacycle *S*-**15**; an intermediate nitrile complex was not observed (Scheme 5). Racemic nitrile (3 equiv) gave a 1.7:1 mixture of diastereomeric metallacycles. The rare M-P-O-C-N ring was characterized by multinuclear NMR spectroscopy.[20] In the $^{31}P\{^1H\}$ NMR spectrum of *S*-**15**, the PMe_2O chemical shift moved dramatically downfield from 86.7 ppm in precursor **9** to 164.9 ppm in the metallacycle, consistent with ring formation.[21] The large ^{195}Pt-^{31}P coupling constant for the Me-FerroLANE P-donor trans to the NH group (3159 Hz; compare 2412 and 2435

Hz for the PMe_2O and other Me-FerroLANE P) indicated the reduced *trans* influence of the metallacycle N-donor.[22] The NMR spectra of the other diastereomer *R*-**15** were similar (see Table 1). The ^{1}H-^{15}N correlation spectrum (HSQC) acquired with natural-abundance ^{15}N (Figure 2) confirmed the assignment of the NH ^{1}H NMR signals at δ 10.36 and 9.73 in CD_2Cl_2 for *R*- and *S*-**15** and provided the ^{15}N chemical shifts (δ 173.7 and 171.4) and the ^{15}N-^{1}H, ^{15}N-^{31}P and ^{15}N-^{195}Pt coupling constants (77, 38, and 240 or 244 Hz, respectively).[23]

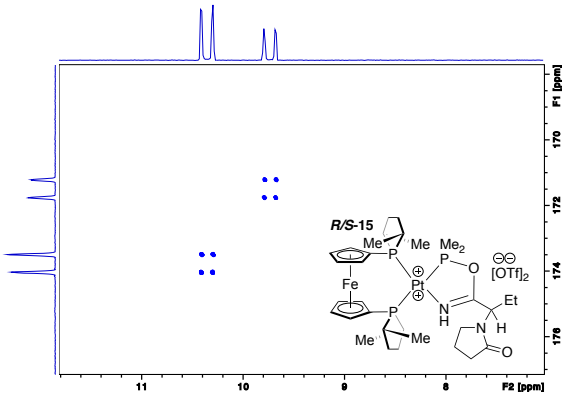

Figure 2. ^{1}H-^{15}N HSQC spectrum (CD_2Cl_2, ^{1}H 700 MHz, ^{15}N 71 MHz) of a diastereomeric mixture of metallacycles **15**.

Notably, when a mixture of dication **9** and 3 equiv of *S*-Keppra nitrile, which generated metallacycle *S*-**15**, was treated with 3 equiv of the racemic nitrile, a 1.4:1 (*S*/*R*) mixture of diastereomeric metallacycles was formed (Scheme 5), suggesting that metallacycle formation was reversible. Related experiments with differing amounts of *S*-nitrile and *rac*-nitrile enabled determination of the approximate equilibrium constant K_{eq} = [*R*-**15**][*S*-nitrile]/[*S*-**15**][*R*-nitrile] ~ 2, showing that one diastereomer of the metallacycle, containing the *R*-nitrile, was favored thermodynamically by a slim margin (K_{eq} ~ 2 at 298 K corresponds to a free energy difference of ca. 0.5 kcal/mol). More reliable measurements of the equilibrium constant were complicated by the tendency of the Pt complexes to scavenge trace water in the solvent or reagents to hydrate the nitriles, as observed by NMR spectroscopy (see below).

Scheme 5. Diastereoselective and reversible formation of metallacycles *R*-**15** and *S*-**15** in reaction of [Pt((*R*,*R*)-Me-FerroLANE)(PMe_2OH)][$OTf]_2$ (**9**) with enantiomerically pure (*S*) or racemic Keppra nitrile

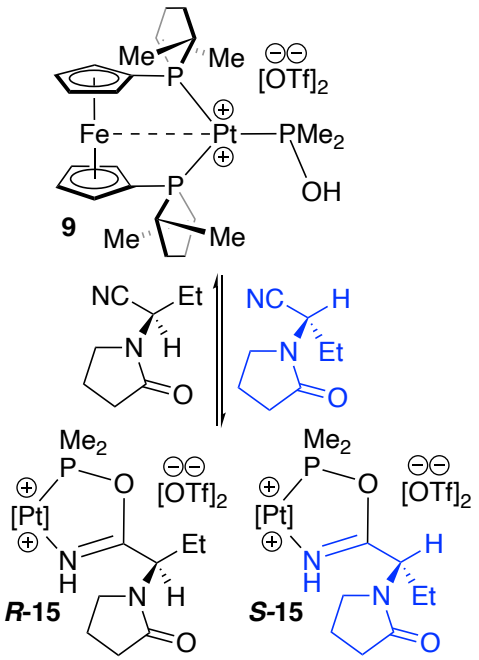

Diastereoselective metallacycle formation was a general process, which also occurred with the other dicationic [Pt(diphos*)(SPO)]$^{2+}$ complexes **10**-**11** or the analogous cation [Pt(*S*,*S*)-Et-FerroTANE)(PMe_2OH)(OTf)]$^{+}$ (**13**) and 3 equiv of racemic Keppra nitrile (Scheme 6). Precursor **14** containing a chiral phosphinous acid ligand formed metallacycles **19** (dr = 1.1). Similarly, treatment of [Pt((*R*,*R*)-Me-FerroLANE)(PMe_2OH)][$OTf]_2$ (**9**) with excess of the racemic nitriles PhCH(R)(CN) (R = Me, Et, *i*-Pr, Cy) or the cyclopropanenitrile $Ph_2CCH_2CH(CN)$ generated **16**-**24**, as established by $^{31}P\{^{1}H\}$ NMR spectroscopy (Scheme 6, Table 1). These reactions were diastereoselective, but preference for one enantiomer of the nitrile was low. Diastereoselectivity was greater with larger nitrile groups, but varying the size of the SPO had little effect. Thus, for 3 equiv of PhCH(R)(CN), the dr values of **20**-**23** were 1, 1.1, 1.2, and 1.3, respectively, increasing with the size of the R group in the order Me < Et < *i*-Pr < Cy. The diastereoselectivity of metallacycle formation with [Pt((*R*,*R*)-Me-FerroLANE)(PR'_2OH)][$OTf]_2$ and the Keppra nitrile was the same (1.7:1) with R' = Me (**9**) or Et (**12**). Similarly, increasing the size of the FerroLANE substituents from Me to Et in PMe_2OH complexes **9** and **10** changed the metallacycle dr only from 1.7 to 1.6, but the *i*-Pr-FerroLANE complex **11** did not react with the nitrile, consistent with its low catalytic activity.

Scheme 6. Diastereoselective formation of metallacycles **15-24** in reactions of cationic [Pt(diphos*)(PR$_2$OH)]$^{2+}$ complexes **9-11** or **14** or [Pt(*S,S*)-Et-FerroTANE)(PMe$_2$OH)(OTf)]$^+$ (**13**) with 3 equiv of racemic Keppra nitrile, or of [Pt((*R,R*)-Me-FerroLANE)(PMe$_2$OH)][OTf]$_2$ (**9**) with excess racemic nitriles PhCH(R)(CN) (3 equiv) or *cyclo*-Ph$_2$CCH$_2$CH(CN) (10 equiv)[a]

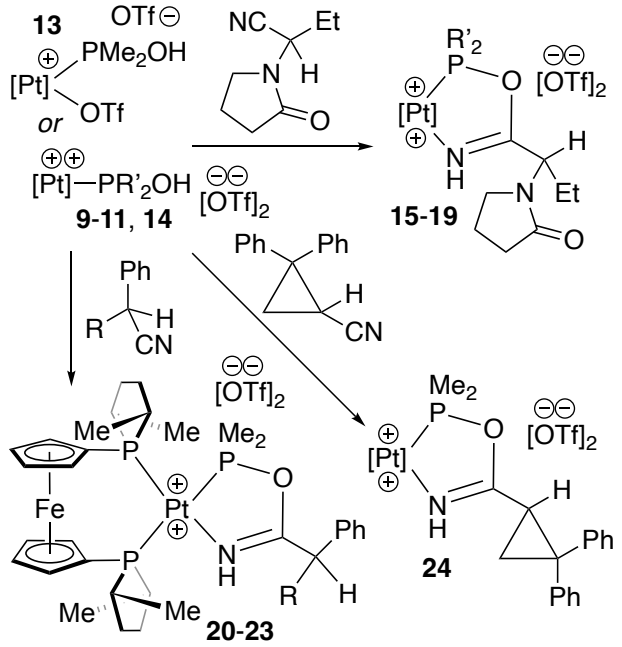

[a] [Pt] = Pt(*R,R*)-Me-FerroLANE, R' = Me for **15** and **20**-**24**, R' = Et for **17**; [Pt] = Pt(*R,R*)-Et-FerroLANE, R' = Me (**16**); [Pt] = Pt(*S,S*)-Et-FerroTANE, R' = Me (**18**); [Pt] = Pt(dppf), PR'$_2$OH = *R*-DMB-P(OH) (**19**); R = Me (**20**), Et (**21**), *i*-Pr (**22**), Cy (**23**)

2. Metallacycle Hydrolysis Gave Unstable Intermediate Iminol Complexes Metallacycles **15**, generated from precursor **9** and racemic or *S*-Keppra nitrile, reacted quickly with water to yield transient intermediates formulated as the iminol complexes **25** (Scheme 7). When one equiv of nitrile and less than one equiv of water was used, some of precursor **9** was reformed. With an excess of nitrile and substoichiometric water (kinetic resolution conditions), intermediates **25** were converted to metallacycles **15** and the Keppra amide. Alternatively, treatment of precursor **9** with an excess of *S*-Keppra amide also generated *S*-**25** in an unfavorable equilibrium; similar Pt-mediated tautomerization processes were observed earlier.[24] This route reproducibly gave *S*-**25**, but unidentified Pt complexes were often also formed. This reaction appeared to be sensitive to the presence of water, but we have not been able to determine the reasons for its variability.

Scheme 7. Generation of iminol complexes **25** by addition of water (or D$_2$O) to metallacycle **15** or from reaction of the Keppra amide with "three-coordinate" precursor **9** ([Pt] = Pt(*R,R*)-Me-FerroLANE)

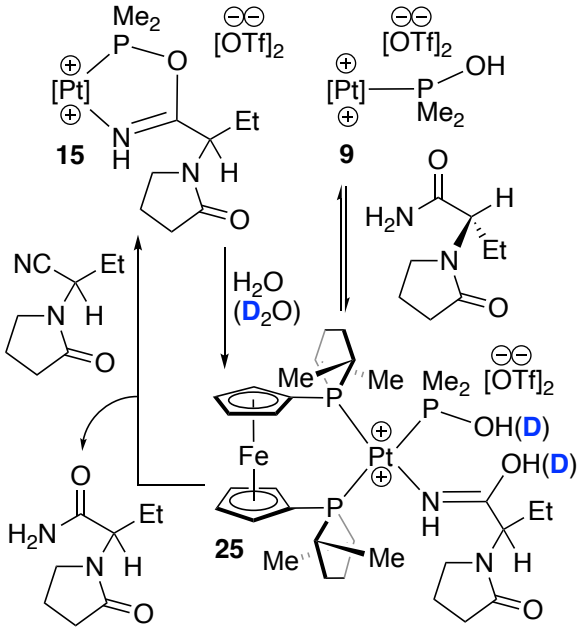

Although complexes **25** could not be isolated, they were identified by ^{31}P{^{1}H} NMR (Table 1) and ^{1}H NMR spectroscopy and by computational studies. Hydrolysis resulted in a drastic change of the PMe$_2$O signal from 164.9 (*S*) or 163.6 (*R*) in metallacycle **15** to 87.2 (*S*) or 88.2 (*R*) ppm in **25**, consistent with ring opening. Both the chemical shifts (22.4 (*S*) and 22.6 (*R*) ppm) and the $J_{Pt\text{-}P}$ coupling constants (3191 and 3149 Hz) for the Me-FerroLANE P trans to the iminol group in **25** were very similar to those in metallacycle **15** (δ 25.0 ($J_{Pt\text{-}P}$ = 3159, *S*) and δ 24.8 ($J_{Pt\text{-}P}$ = 3144, *R*)). The ^{1}H NMR spectrum of **25** in CD$_2$Cl$_2$ included signals assigned to NH groups at 9.0 (*S*) and 9.6 (*R*) ppm, similar to those in precursor **15** at 9.73 (*S*) and 10.36 (*R*) ppm, with P-OH peaks at 10.0 (*S*) and 10.3 (*R*) ppm. Low-field ^{1}H NMR signals at 15.0 (*S*) and 15.3 (*R*) ppm were assigned to the iminol C-OH groups. These spectroscopic observations are similar to previous ones on Pt-iminol complexes, including those formed by nitrile hydration, in which NH and C-OH ^{1}H NMR chemical shifts appeared from ca. 6.5-9.5 ppm and 10-13 ppm, respectively.[24] These assignments are also consistent with the ^{1}H NMR spectrum of *S*-**25** computed with density functional theory (DFT; see the SI for details), which included signals at 15.14 (C-OH), 8.83 (P-OH), and 7.56 (NH) ppm. The unusual iminol ^{1}H NMR chemical shift is consistent with the computed structure of **25** (Chart 1 and SI), which included a hydrogen-bonding chelate interaction between two S-O groups in a triflate anion and the P-OH (SPO) and C-OH (iminol) donors.[25]

When a mixture of metallacycle *S*-**15** and iminol complex *S*-**25**, generated from **9** and the S-Keppra nitrile and residual water in the CD$_2$Cl$_2$ solvent, was treated with one equiv of D$_2$O, the ^{1}H NMR spectrum of the resulting mixture included the 9.0 ppm NH signal, while the δ 15.0 and 10.0 peaks assigned to C-OH and P-OH protons were absent, consistent with attack of D$_2$O at phosphorus in

15 to yield C-OD and P-OD groups (see section 3 below for complementary experiments with $^{18}OH_2$ which reached the same conclusion). The δ 9.0 signal also disappeared in similar experiments with more D_2O and/or longer reaction times, suggesting faster exchange for the C-OH/P-OH sites in comparison to the NH one.

Because complexes **25** were formed in mixtures and decomposed in solution, we were not able to obtain definitive NMR evidence for the proposed iminol ligand, or to rule out the alternative structures of N-bound or O-bound amide complexes (Chart 1), which could be formed by tautomerization of an iminol complex. DFT calculations (B3LYP-D3/LACV3P**+/CH_2Cl_2) on these three isomeric complexes including the triflate anions and the *S*-enantiomer of the iminol/amide showed that the iminol complex was lowest in energy in the gas phase, consistent with previous examples of amide/iminol tautomerism at Pt,[24] but the O-bound amide complex was preferred in CH_2Cl_2 (see the relative free energies in Chart 1). The computed structures of the O-bound or N-bound amide complexes included P-OH-triflate H-bonding, as in the iminol complex. The other triflates were found near the Pt(Me-FerroLANE) groups.

Although these results ruled out the high-energy N-bound amide complex, the similar energies of the iminol and O-bound amide complexes, as well as formation of *S*-**25** from the amide, made structural assignment challenging. However, the computed ^{1}H NMR spectra for the amide complexes (see the SI) did not match the experimental observations well. In particular, they were not able to reproduce the 15-ppm signal assigned to a C-OH group; in the computed spectrum for the O-bound amide complex, the closest resonance was a P-OH peak at 10.2 ppm. From these experimental and computational results, we formulate **25** as an iminol complex. However (see below), the O-bound amide complex tautomer may also be involved in catalysis en route to Keppra amide formation.

Chart 1. Computed Structures (DFT/B3LYP-D3/LACV3P**+/CH_2Cl_2) and Relative Free Energies (kcal/mol) of Iminol, O-Bound Amide, and N-Bound Amide Isomers of Intermediate *S*-**25**. Relative Free Energies Are Listed in the Gas Phase (Plain Text) and in CH_2Cl_2 (Italics).

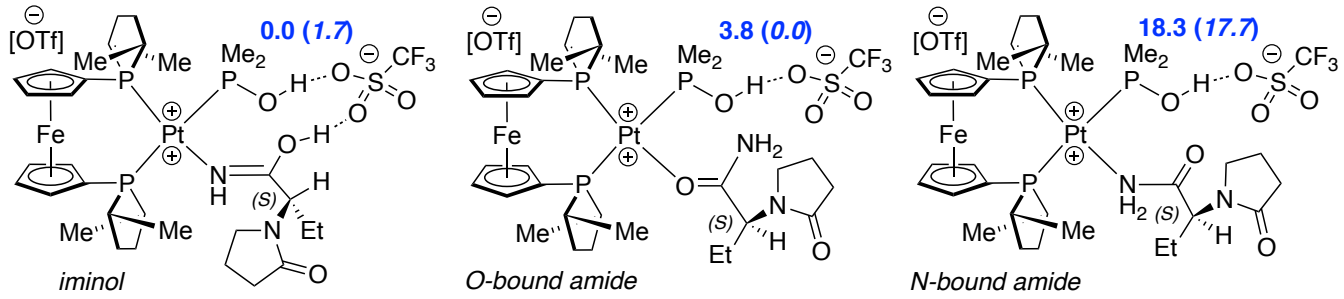

3. Metallacycle Hydrolysis via Water Attack at PMe_2O Phosphorus: $^{31}P\{^1H\}$ NMR Evidence from ^{18}O-Labeling Iminol complex *S*-**25** was presumably formed by attack of water at the metallacycle PMe_2O group in **15**,[11] which was confirmed using $^{18}OH_2$ by perturbation of the ^{31}P NMR chemical shift of the resulting ^{31}P-^{18}O group (Scheme 8).[26] For example, Figure 3 shows a portion of the $^{31}P\{^1H\}$ NMR spectrum of a mixture of metallacycle *S*-**15** and excess Keppra nitrile after treatment with half an equiv of $^{18}OH_2$. Reaction of the nitrile with the resulting iminol complex then gave the amide and a mixture of metallacycle isotopologues with distinct chemical shifts. The apparent doublet of triplets pattern arises from overlapping doublet of doublet signals for *S*-**15** and *S*-**15**-^{18}O. Please see the SI for additional details of ^{18}O-labeling experiments.

Scheme 8. Reaction of metallacycle **15** with water ($^{16}OH_2$, $^{18}OH_2$, or mixtures) to generate iminol complex **25**, with formation of the Keppra amide and regeneration of **15** from excess nitrile ([Pt] = Pt(*R*,*R*)-Me-FerroLANE)

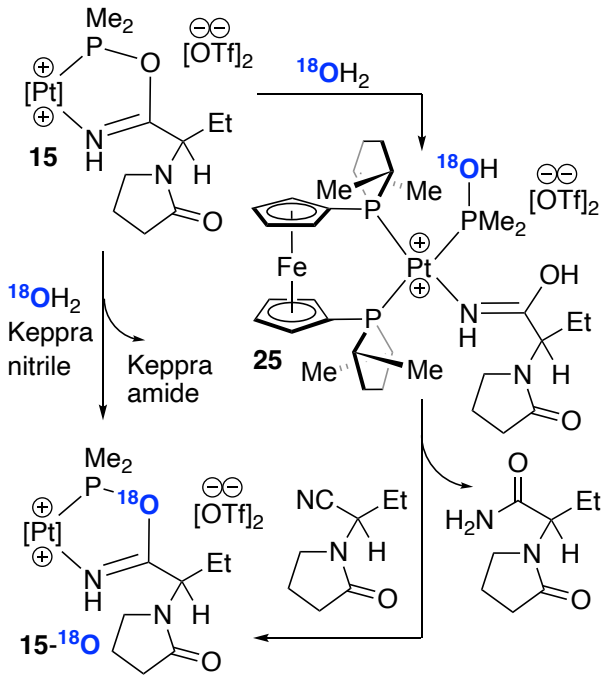

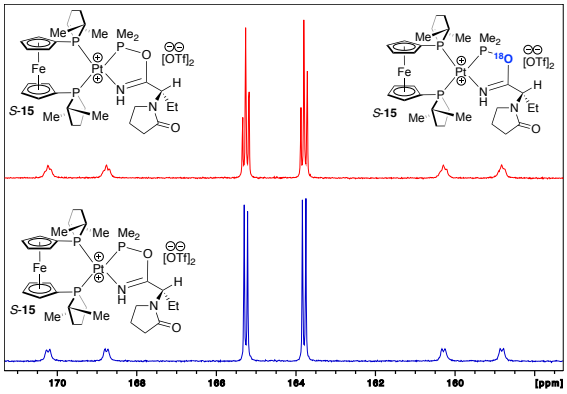

Figure 3. A portion of the $^{31}P\{^{1}H\}$ NMR spectrum (CD_2Cl_2, 243 MHz) of a mixture of metallacycle *S*-**15** (below, blue) and excess Keppra nitrile after treatment with 0.5 equiv of $^{18}OH_2$, showing overlapping signals due to ^{18}O- and ^{16}O-containing metallacycles *S*-**15** (above, red)

In contrast, reaction of water with the metallacycle [Pt(dppf)(PMe_2OC(*p*-I-C_6H_4)=NH)][OTf]$_2$ was reported to directly yield the amide and the aquo complex [Pt(dppf)(PMe_2OH)(H_2O)][OTf]$_2$.[11] However, an unassigned minor doublet signal ($\delta \sim 90$) in the $^{31}P\{^{1}H\}$ NMR spectrum of that reaction mixture may be due to a Pt-PMe_2OH group in an intermediate iminol complex. We generated the analogous aquo complex **26** in an apparent equilibrium mixture ($K_{eq} \sim 1$) from reaction of precursor **9** with water (Scheme 9) and characterized it by NMR spectroscopy (Table 1). This intermediate was not observed in catalysis or stoichiometric reactions in the presence of excess nitrile.

Scheme 9. Generation of aquo complex **26**

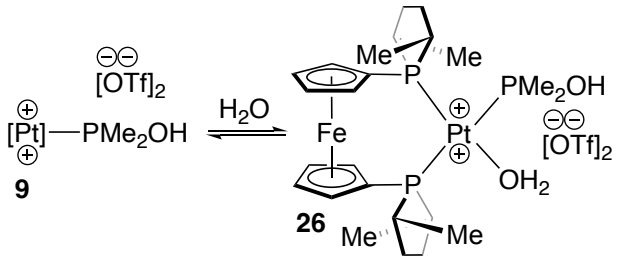

4. Proposed Mechanism of Pt(PR_2OH)-Catalyzed Nitrile Hydration On the basis of the stoichiometric reactions, Scheme 10 shows a proposed mechanism for hydration of the Keppra nitrile catalyzed by [Pt((*R*,*R*)-Me-FerroLANE)(PMe_2OH)]$^{2+}$ precursor **9**, which we hypothesize also applies to related processes. As in Scheme 2, identical cycles for the enantiomeric substrates are shown in blue (*R*) and black (*S*). Reaction of **9** with the nitrile substrate gave metallacycles **15** in a modestly diastereoselective process, which presumably occurred via the unobserved nitrile complexes **28**. Addition of racemic or *S*-Keppra nitrile to **15** resulted in a change in the diastereomeric ratio, suggesting that both metallacycle formation and nitrile binding in **28** were reversible, and that diastereoselectivity in metallacycle formation was under thermodynamic control. Attack of water at the PMe_2O phosphorus in the metallacycle then generated iminol complexes **25**, and ligand substitution with the nitrile gave the amide product and regenerated the metallacycle. This process might be associative, with nitrile attack on **25**, or dissociative, via loss of iminol (or amide), which could be promoted by coordination of iron to yield precursor **9**.[17c]

Iminol-amide tautomerization might occur either on or off the metal. Although we have formulated intermediates **25** as the initial product of metallacycle hydrolysis, iminol complexes, we cannot rule out the alternative O-bound amide complexes, which could also be on the reaction pathway en route to the Keppra amide. The isotope effect (slower catalytic reaction with D_2O vs H_2O) suggested that the rate-determining step was proton transfer, occurring after reaction of water with the metallacycle either in formation of the iminol complex or in tautomerization.[27]

Scheme 10. Proposed Mechanism of Hydration of the Keppra Nitrile by the Catalyst Precursor [Pt(*R,R*)-Me-FerroLANE)(PMe$_2$OH)][OTf]$_2$ (**9**), with Reversible Formation of Metallacycles **15** and Their Attack by Water at the PMe$_2$O Phosphorus to Yield Iminol Complexes **25**, Followed By Catalytic Turnover to Form the Keppra Amide ([Pt] = Pt(*R,R*)-Me-FerroLANE))

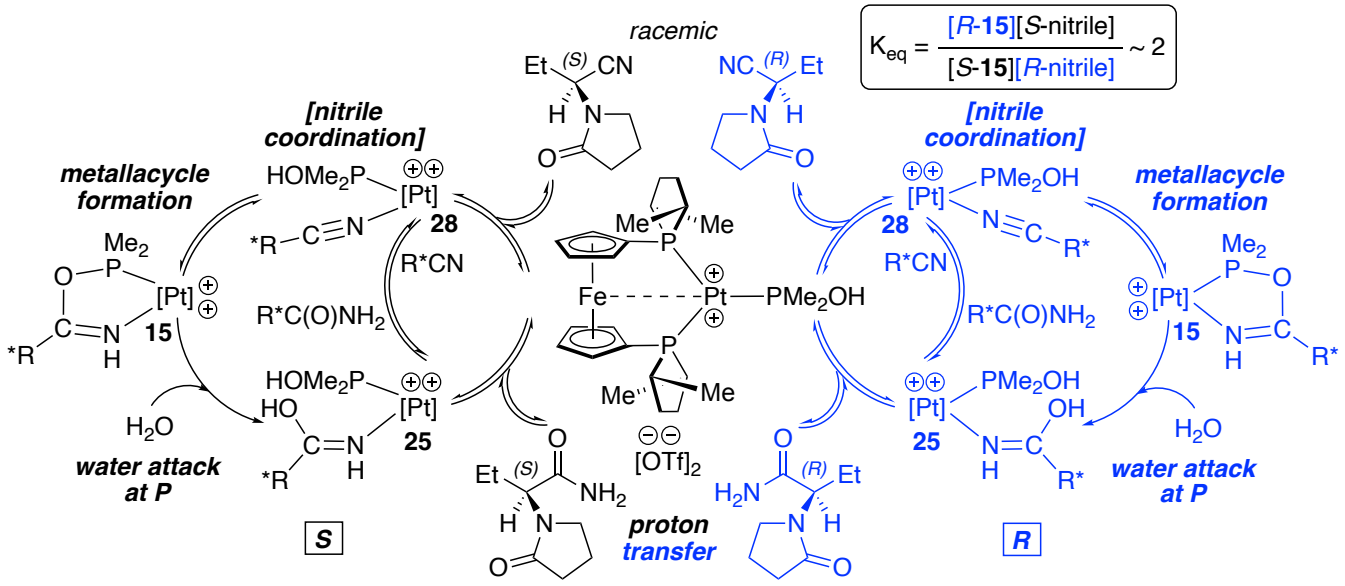

CONCLUSIONS

This study has provided fundamental information on the proposed mechanism of Scheme 2 and yielded nitrile hydration catalysts which operate quickly at room temperature. Variation of catalyst structure showed that the least sterically demanding ligand (Me-FerroLANE) and nucleophile (PMe$_2$OH) yielded the fastest catalysts. We have confirmed the hypothesis that metallacycle formation can be diastereoselective with a chiral ligand and showed that this process is reversible. Observation of iminol complex **25** and ^{18}O-labeling studies demonstrated that water attacks at the metallacycle PMe$_2$O phosphorus to complete nitrile hydration mediated by the bifunctional phosphinous acid ligand. The same mechanistic conclusion was reached previously with the [Pt(dppf)(PMe$_2$OH)]$^{2+}$ catalyst by mass spectrometric studies using ^{18}OH$_2$.[11] The new features of this study include observation of the hydrolysis intermediate iminol complexes **25** and the reversibility and diastereoselectivity of metallacycle formation.

If metallacycle formation is diastereoselective, why was kinetic resolution in hydration of the Keppra nitrile not enantioselective? We hypothesize that initial nitrile binding in **28** and formation of metallacycles **15** was kinetically unselective, because the nitrile stereocenter was remote from the diphos* ligand. If irreversible attack of water on **15** (rate constant k' in Scheme 2) was faster than equilibration of the diastereomeric metallacycles (rate constant k in Scheme 2), then the (presumably low) kinetic ratio of metallacycles would be retained in the product amide. Design of improved catalysts should therefore focus on improving the kinetic selectivity of one or more of the key steps of nitrile coordination, metallacycle formation, and water attack. Future studies will focus on chiral SPO preligands, with the goal of making metallacycle formation and decomposition more selective. This approach was adopted in the only previous non-biological example of asymmetric nitrile hydration[6] and may benefit from recent progress in the synthesis of chiral SPOs.[28] Although it is more sterically demanding than PMe$_2$OH, the binaphthyl-based phosphinous acid in precursor **14** generated an active, albeit unselective catalyst. Replacing the achiral dppf in **14** with a chiral diphos* ligand may improve the selectivity of kinetic resolution in catalytic hydration of racemic nitriles.

EXPERIMENTAL SECTION

General Experimental Details. Unless otherwise noted, all reactions and manipulations were performed under nitrogen using glovebox and Schlenk techniques at ambient temperature. Anhydrous pentane, CH_2Cl_2, ether, THF, and toluene were dried further over molecular sieves, which were oven dried and then dried under vacuum over 6 h at 200 °C, or at 120 °C for 12 h. Celite used for filtration was dried under vacuum for 4 h. NMR spectra were recorded by using a 600 MHz spectrometer. ^{1}H or ^{13}C NMR chemical shifts are reported vs Me$_4$Si and were determined by reference to the residual ^{1}H or ^{13}C solvent peaks. ^{31}P NMR chemical shifts are reported vs H_3PO_4 (85%) used as an external reference. ^{19}F NMR chemical shifts are reported vs $CFCl_3$. Coupling constants are reported in Hz, as absolute values. Unless indicated, peaks in NMR spectra are singlets. Mass spectrometry was performed at the University of Illinois. Elemental analysis was carried out by Atlantic Microlab, Norcross, GA. Unless otherwise noted, reagents were from commercial suppliers. These compounds were prepared by literature procedures: Pt((*R,R*)-Me-FerroLANE)Cl$_2$, Pt((*R,R*)-Et-FerroLANE)Cl$_2$, Pt((*R,R*)-*i*-Pr-FerroLANE)Cl$_2$, Pt((*R,R*)-Et-FerroTANE)Cl$_2$,[14] Pt(dppf)Cl$_2$,[29] *R*-DMB-PH(O),[6] and the cations [Pt((*R,R*)-Me-FerroLANE)(PMe$_2$OH)(Cl)][OTf] (**1**) and [Pt((*R,R*)-Me-FerroLANE)(PMe$_2$OH)][OTf]$_2$ (**9**).[15] As described in the SI, enantiomerically enriched *S*-Keppra nitrile was prepared from the commercially available amide by modification of a literature procedure,[19] and its base-mediated racemization gave racemic Keppra nitrile.[5b]

[Pt((*R,R*)-Me-FerroLANE)(PEt$_2$OH)(Cl)][OTf] (**2**) An orange CH_2Cl_2 solution of freshly prepared Pt((*R,R*)-Me-FerroLANE)Cl$_2$ (121.3 mg, 0.178 mmol) and PEt$_2$Cl (23.3 mg, 0.187 mmol, 1.1 equiv) was added to solid AgOTf (98%, 48.1 mg, 0.183 mmol, 1.1 equiv). A white precipitate appeared. The mixture was protected from light and stirred overnight. The ^{31}P{^{1}H} NMR spectrum of the reaction mixture showed full conversion to an intermediate, presumably [Pt((*R,R*)-Me-FerroLANE)(PEt$_2$Cl)(Cl)][OTf] [**7**, ^{31}P{^{1}H} NMR (243 MHz, $CDCl_3$): δ

118.6 (dd, J_{Pt-P} = 2492, $J_{P-P\ trans}$ = 455, $J_{P-P\ cis}$ = 23), 39.5 (d, J_{Pt-P} = 2548, $J_{P-P\ trans}$ = 455, $J_{P-P\ cis}$ = 9), 39.5 (d, J_{Pt-P} = 3581, $J_{P-P\ cis}$ = 22, $J_{P-P\ cis}$ = 10)].

Then, outside of the glovebox, distilled water (3.4 μL, 1.1 equiv) was added and the mixture was stirred at room temperature overnight. The $^{31}P\{^{1}H\}$ NMR spectrum of the reaction mixture showed conversion to a mixture of residual [Pt((*R,R*)-Me-FerroLANE)(PEt_2Cl)(Cl)][OTf] (6%), Pt((*R,R*)-Me-FerroLANE)Cl_2 (47%; δ_P 30 (J_{Pt-P} = 3690)), and what is apparently the SPO $PHEt_2(O)$ (47%, δ_P 65.2, J_{P-H} = 509; note that this chemical shift does not match the literature value of 42.8 ppm ($CDCl_3$),[30] perhaps because of interaction with HOTf formed by hydrolysis of PEt_2Cl in the presence of triflate anion).

Then, the solvent was removed with a rotary evaporator and the residue was taken back into the glovebox. The yellow residue was suspended in THF and then a THF solution of AgOTf (50 mg, 0.19 mmol) was added dropwise. The reaction mixture was stirred for 1 h at room temperature and then 1 h at 60 °C to give a yellow solution with a white and purple precipitate. The solvent and volatiles were removed under vacuum. The residue was extracted with minimal CH_2Cl_2 and the resulting solution was filtered through a Celite column. Solvent was removed under vacuum and the residue was triturated and washed with pentane to give a yellow powder. Crystals were obtained from a concentrated CH_2Cl_2 solution of the yellow powder layered with pentane at -20 °C (70 mg, 44%). The $^{31}P\{^{1}H\}$ NMR spectrum of these crystals revealed partial formation (<10%) of 3-coordinate [Pt((*R,R*)-Me-FerroLANE)(PEt_2OH)][OTf]$_2$ (**10**, see below; δ_P 112.4 (br, J_{Pt-P} = 4455), 19.0 (d, J_{Pt-P} = 2229, $J_{P-P\ cis}$ = 11)); note that elemental analysis data was obtained for this mixture.

Anal. calcd. for $C_{27}H_{43}ClF_3FeO_4P_3PtS$: C, 36.03; H, 4.82. Found: C, 35.76; H, 4.95. HRMS (ESI+) calcd. for $[C_{26}H_{43}ClFeOP_3Pt]^+$ (M^+): 750.1213, Found 750.1244. $^{31}P\{^{1}H\}$ NMR (243 MHz, CD_2Cl_2): δ 113.1 (dd, J_{Pt-P} = 2799, $J_{P-P\ trans}$ = 438, $J_{P-P\ cis}$ = 24), 37.9 (dd, J_{Pt-P} = 2148, $J_{P-P\ trans}$ = 438, $J_{P-P\ cis}$ = 12), 37.8 (dd, J_{Pt-P} = 3646, $J_{P-P\ cis}$ = 24, $J_{P-P\ cis}$ = 12). ^{1}H NMR (600 MHz, CD_2Cl_2): δ 8.81 (1H, OH), 4.70 (d, *J* = 7, 2H, CH Cp), 4.54 (br, 2H, CH Cp), 4.38 (br, 1H, CH Cp), 4.28 (d, *J* = 6, 2H, CH Cp), 4.23 (br, 1H, CH Cp), 3.55-3.43 (m, 2H, CH), 2.89-2.81 (m, 1H, CH), 2.80-2.71 (m, 1H, CH), 2.70-2.60 (m, 1H, CH_2 P*Et*$_2$OH), 2.46-2.32 (m, 2H, CH_2 phospholane + CH_2 P*Et*$_2$OH), 2.31-2.16 (m, 3H, CH_2 phospholane + CH_2 P*Et*$_2$OH), 2.15-1.93 (m, 2H, CH_2), 1.82-1.74 (m, 1H, CH_2), 1.74-1.69 (m, 1H, CH_2), 1.67 (dd, *J* = 19, 7, 3H, CH_3), 1.61 (dd, *J* = 20, 7, 3H, CH_3), 1.49-1.23 [m, 10H overlaps 4H, CH_2 phospholane + 1.37 (dt, *J* = 19, 8, 3H, CH_3 P*Et*$_2$OH) + 1.30 (dt, *J* = 20, 8, 3H, CH_3 P*Et*$_2$OH)], 0.97 (dd, *J* = 16, 7, 3H, CH_3), 0.81 (dd, *J* = 17, 7, 3H, CH_3). $^{13}C\{^{1}H\}$ NMR (151 MHz, CD_2Cl_2): δ 76.4 (d, *J* = 8, CH Cp), 76.1 (br, CH Cp), 75.5 (d, J = 9, CH Cp), 74.9 (d, *J* = 4, CH Cp), 74.7 (d, *J* = 15, CH Cp), 74.2 (d, *J* = 4, CH Cp), 74.1 (br, CH Cp), 73.7 (d, *J* = 5, CH Cp), 38.3 (dd, *J* = 39, 5, CH), 37.7 (d, *J* = 33, CH), 37.5 (br, CH_2), 35.8 (dd, *J* = 31, 3, CH), 35.5 (d, *J* = 3, CH_2), 35.3 (d, *J* = 3, CH_2), 35.1 (d, *J* = 34, CH), 34.8 (d, *J* = 4, CH_2), 25.7 (dd, *J* = 42, 2, CH_2 P*Et*$_2$OH), 25.4 (dd, *J* = 34, 5, CH_2 P*Et*$_2$OH), 20.9 (d, *J* = 6, CH_3), 20.0 (d, *J* = 7, CH_3), 14.7 (CH_3), 14.4 (CH_3), 8.4 (CH_3 P*Et*$_2$OH), 8.2 (d, *J* = 3, CH_3 P*Et*$_2$OH). The quaternary Cp signals were not observed. $^{19}F\{^{1}H\}$ NMR (565 MHz, CD_2Cl_2): δ -78.8.

[Pt((*R,R*)-Et-FerroLANE)(PMe_2OH)(Cl)][OTf] (3). To a bright orange THF solution of freshly prepared Pt((*R,R*)-Et-FerroLANE)Cl_2 (61.4 mg, 0.083 mmol) and PMe_2OH (95%, 8.2 mg, 0.11 mmol, 1.2 equiv), a THF solution of AgOTf (39.3 mg, 0.153 mmol, 1 equiv) was added dropwise. A white precipitate appeared. The mixture was stirred in an oil bath at 60 °C for 1 h. After cooling to room temperature, the solvent and volatiles were removed under vacuum. The residue was extracted with minimal CH_2Cl_2 and the resulting solution was filtered through a Celite column. The solvent was removed under reduced pressure and the yellow residue was washed with pentane to give a yellow powder. The powder was dissolved in minimal CH_2Cl_2 and the solution was layered with pentane and stored in the freezer at –20 °C for over a week to give a precipitate, which was decanted, washed with pentane, and dried under vacuum for 1 h (59 mg, 77%).

HRMS (ESI+) m/z calcd for $[C_{28}H_{47}ClFeOP_3Pt]^+$: 778.1525; Found, 778.1532. $^{31}P\{^{1}H\}$ NMR (243 MHz, CD_2Cl_2): δ 95.8 (dd, J_{Pt-P} = 2794, $J_{P-P\ trans}$ = 458, $J_{P-P\ cis}$ = 26), 34.2 (dd, J_{Pt-P} = 2156, $J_{P-P\ trans}$ = 458, $J_{P-P\ cis}$ = 11), 32.4 (dd, J_{Pt-P} = 3623, $J_{P-P\ cis}$ = 27, $J_{P-P\ cis}$ = 11). ^{1}H NMR (600 MHz, CD_2Cl_2): δ 9.18 (br, 1H, OH), 4.68 (d, *J* = 8, 2H, CH Cp), 4.53 (2H, CH Cp), 4.35 (1H, CH Cp), 4.28 (1H, CH Cp), 4.24 (2H, CH Cp), 3.36-3.30 (m, 2H), 2.58-2.43 (m, 3H), 2.36-2.21 (m, 2H), 2.20-1.95 (m, 11H), 1.73-1.65 (m, 1H), 1.54-1.47 (m, 1H), 1.37-1.24 (m, 5H), 1.22-1.07 (m, 13H).

[Pt((*R,R*)-*i*-Pr-FerroLANE)(PMe_2OH)(Cl)][OTf] (4) An orange CH_2Cl_2 solution of freshly prepared Pt((*R,R*)-*i*-Pr-FerroLANE)Cl_2 (100 mg, 0.126 mmol) and PMe_2Cl (97%, 15.2 mg, 0.152 mmol, 1.2 equiv) was added to solid AgOTf (98%, 34.9 mg, 0.133 mmol, 1.1 equiv). A white precipitate appeared. The mixture was covered from light and stirred overnight. The $^{31}P\{^{1}H\}$ NMR spectrum of the reaction mixture showed full conversion to the intermediate cation [Pt((*R,R*)-Me-FerroLANE)(PMe_2Cl)(Cl)][OTf] (**8**, $^{31}P\{^{1}H\}$ NMR (243 MHz, $CDCl_3$): δ 87.8 (dd, J_{Pt-P} = 2484, $J_{P-P\ trans}$ = 479, $J_{P-P\ cis}$ = 26), 29.4 (d, J_{Pt-P} = 2591, $J_{P-P\ trans}$ = 480), 20.3 (d, J_{Pt-P} = 3560, $J_{P-P\ cis}$ = 25)). Then, outside of the glovebox, distilled water (10 μL, 4.4 equiv) was added and the mixture was stirred at room temperature overnight. The solvent and volatiles were removed under vacuum. The residue was extracted with minimal CH_2Cl_2 and the resulting solution was filtered through a Celite column. Solvent was removed under vacuum and the oily residue was triturated and washed with pentane to give a yellow powder that was dried under vacuum for 4 h (105 mg, 85%). We were not able to grow crystals from CH_2Cl_2/pentane mixtures.

Anal. Calcd. for $C_{33}H_{55}ClF_3FeO_4P_3PtS$: C, 40.27; H, 5.63. Found: C, 41.02; H, 5.80. HRMS (ESI+) m/z calcd. for $[C_{32}H_{55}ClFeOP_3Pt]^+$ (M^+): 834.2151, Found 834.2150. $^{31}P\{^{1}H\}$ NMR (243 MHz, CD_2Cl_2): δ 91.5 (dd, J_{Pt-P} = 2821, $J_{P-P\ trans}$ = 456, $J_{P-P\ cis}$ = 28), 29.2 (dd, J_{Pt-P} = 2147, $J_{P-P\ trans}$ = 456, $J_{P-P\ cis}$ = 10), 19.8 (dd, J_{Pt-P} = 3613, $J_{P-P\ cis}$ = 28, $J_{P-P\ cis}$ = 10). ^{1}H NMR (600 MHz, CD_2Cl_2): δ 9.41 (br, 1H, OH), 4.69 (br, 1H, CH Cp), 4.66 (br, 1H, CH Cp), 4.65 (br, 1H, CH Cp), 4.49 (br, 2H, CH Cp), 4.43 (1H, CH Cp), 4.29 (br, 1H, CH Cp), 4.25 (br, 1H, CH Cp), 3.30-3.22 (m, 1H, CH), 3.22-3.14 (m, 1H, CH), 2.75-2.66 (m, 1H, CH *i*-Pr), 2.59-2.54 (m, 1H, CH), 2.42-2.33 (m, 2H, CH phospholane + CH *i*-Pr), 2.25-2.06 [m, 10H overlaps 2.25-2.14 (m, 4H, CH_2 phospholane) + 2.11 (apparent t, 6H, CH_3 P*Me*$_2$OH)], 2.06-1.94 (m, 2H, CH_2), 1.75 (d, *J* = 6, 3H CH_3 *i*-Pr), 1.73-1.64 (m, 3H, CH *i*-Pr + CH_2), 1.44-1.34 [m, 7H overlaps 1H, CH *i*-Pr + 1.42 (d, *J* = 7, 3H, CH_3 *i*-Pr) + 1.39-1.36 (m, 3H, CH_3 *i*-Pr)], 1.20 (d, *J* = 7, 3H, CH_3 *i*-Pr), 1.17 (d, *J* = 7, 3H, CH_3 *i*-Pr), 1.14 (d, *J* = 6, 3H, CH_3 *i*-Pr), 0.81 (d, *J* = 6, 6H, CH_3 *i*-Pr). $^{13}C\{^{1}H\}$ NMR (151 MHz, CD_2Cl_2): δ 75.9 (d, *J* = 8, CH Cp), 75.3 (d, *J* = 9, CH Cp), 75.1 (d, *J* = 3, CH Cp), 74.5 (br, CH Cp), 74.3 (br, CH Cp), 73.9 (d, *J* = 4, CH Cp), 73.6 (d, *J* = 13, CH Cp), 73.0 (d, *J* = 5, CH Cp), 50.3 (d, *J* = 36, CH), 48.2 (d, *J* = 37, CH), 48.0 (dd, *J* = 27, 4, CH), 47.6 (d, *J* = 30, CH), 32.2 (d, *J* = 3, CH *i*-Pr), 31.5 (d, *J* = 7, CH *i*-Pr), 30.7-30.5 (m, CH_2), 30.5-30.3 (m, CH_2), 30.0-29.8 (m, CH_2), 28.4 (br, CH *i*-Pr), 27.7 (d, *J* = 6, CH_3 *i*-Pr), 26.4 (d, *J* = 11, CH_3 *i*-Pr), 24.9 (CH_3 *i*-Pr), 24.8 (CH_3 *i*-Pr), 22.0 (d, *J* = 11, CH_3 *i*-Pr), 21.8 (d, *J* = 10, CH_3 *i*-Pr), 21.6 (d, *J* = 10, CH_3 *i*-Pr), 20.6 (dd, *J* = 24, 3, CH_3 P*Me*$_2$OH), 20.4 (dd, *J* = 23, 4, CH_3 P*Me*$_2$OH), 19.8 (d, *J* = 5, CH_3 *i*-Pr). The quaternary Cp signals were not observed. $^{19}F\{^{1}H\}$ NMR (565 MHz, CD_2Cl_2): δ -78.9.

[Pt((*S,S*)-Et-FerroTANE)(PMe_2OH)(Cl)][OTf] (5) To a bright orange THF solution of freshly prepared Pt((*S,S*)-Et-FerroTANE)Cl_2 (171.4 mg, 0.242 mmol) and $PHMe_2(O)$ (95%, 23.9 mg, 0.306 mmol, 1.3 equiv), a THF solution of AgOTf (98%, 68.4 mg, 0.261 mmol, 1.1 equiv) was added dropwise. A white precipitate appeared. The mixture was stirred magnetically in an oil bath at 60 °C for 1 h. After cooling to room temperature, the solvent and volatiles were removed under vacuum. The residue was extracted with minimum CH_2Cl_2 and the resulting solution was filtered through a Celite column. The filtrate was concentrated, layered with pentane, and stored in the freezer at –30 °C for over one week. A yellow precipitate was decanted from the liquor, washed with pentane, and dried under vacuum (18 mg, 8%).

Anal. Calcd. for $C_{27}H_{43}ClF_3FeO_4P_3PtS$: C, 36.03; H, 4.82. Found: C, 36.29; H, 4.99. HRMS (ESI+) calcd. for $[C_{26}H_{43}ClFeOP_3Pt]^+$: 750.1212, Found 750.1207. HRMS (ESI+) calcd. for $[C_{26}H_{43}ClFeOP_3Pt]^+$ – HCl: 714.1446, Found 714.1448. $^{31}P\{^{1}H\}$ NMR (243 MHz, CD_2Cl_2) δ 94.8 (br d, J_{Pt-P} = 2813, $J_{P-P\ trans}$ = 438), 40.5 (br d, J_{Pt-P} = 1973, $J_{P-P\ trans}$ = 438), 36.7 (br, J_{Pt-P} = 3374). ^{1}H NMR (600 MHz, CD_2Cl_2): δ 9.01 (1H, OH), 4.77

(br, 2H, CH Cp), 4.65 (br, 2H, CH Cp), 4.62 (br, 2H, CH Cp), 4.38–4.33 (m, 2H, CH Cp), 3.96 (br, 1H, CH), 3.85–3.76 (m, 1H, CH), 2.77–2.59 (m, 4H, overlap CH + CH_2), 2.43–2.30 (m, 2H, CH_2), 2.30–2.22 (m, 1H, CH_2), 2.21–2.05 (m, 7H, overlap CH_3 PMe_2OH (2.18 (d, J = 9, 3H), 2.12 (d, J = 11, 3H) + 1H CH_2), 2.04–1.88 (m, 2H, CH_2), 1.37–1.15 (m, 10H, overlap CH_3 + CH_2), 0.76 (m, 6H, CH_3). $^{13}C\{^1H\}$ NMR (151 MHz, CD_2Cl_2): δ 76.8 (d, *J* = 14, CH Cp), 76.2 (d, *J* = 8, CH Cp), 75.8 (d, *J* = 6, CH Cp), 75.6 (d, *J* = 11, CH Cp), 74.3 (d, *J* = 6, CH Cp), 74.2 (d, *J* = 6, CH Cp), 74.0 (d, *J* = 5, CH Cp), 73.9 (vt, *J* = 4, CH Cp), 68.7 (d, *J* = 52, quat Cp), 65.6–65.2 (br, quat Cp), 40.9 (d, *J* = 43, CH), 40.6 (br d, *J* = 38, CH), 40.0 (d, *J* = 37, CH), 35.8 (dd, *J* = 16, 5, CH_2), 35.4 (d, *J* = 36, CH), 34.8 (d, *J* = 16, CH_2), 27.2–26.9 (m, CH_2), 25.7 (d, *J* = 2, CH_2), 24.9 (d, *J* = 6, CH_2), 24.8 (d, *J* = 5, CH_2), 21.0 (d, *J* = 40, CH_3 P*Me*$_2$OH), 20.1 (d, *J* = 39, CH_3 P*Me*$_2$OH), 14.1 (d, *J* = 11, CH_3), 13.7 (d, *J* = 13, CH_3), 12.0 (d, *J* = 10, CH_3), 11.9 (d, *J* = 13, CH_3). $^{19}F\{^1H\}$ NMR (565 MHz, CD_2Cl_2) δ -78.9.

[Pt(dppf)(*R*-DMB-P(OH))(Cl)][OTf] (6) A Schlenk flask was loaded with Pt(dppf)Cl_2 (119 mg, 0.145 mmol) suspended in THF, a colorless THF solution of the *R*-DMB-SPO (50 mg, 0.15 mmol, 1.1 equiv), and a colorless THF solution of AgOTf (98%, 41.7 mg, 0.159 mmol, 1.1 equiv). A white precipitate appeared. The mixture was stirred for 1 h at 60 °C. The solvent and volatiles were removed under vacuum. The residue was extracted with minimal CH_2Cl_2 and the resulting solution was filtered through a Celite column. Solvent was removed under vacuum and the residue was washed with pentane to give a yellow powder that was dried under vacuum for 2 h. This solid was dissolved again in minimal CH_2Cl_2, layered with pentane, and stored in the freezer overnight at –20 °C to form a yellow oil, which was decanted, washed and triturated with pentane, and dried under vacuum for 2 h to give a yellow powder (120 mg, 66%).

HRMS (ESI+) m/z calcd. for $[C_{56}H_{44}FeOP_3Pt]^+$ $(M–HCl)^+$: 1076.1602; Found: 1076.1599. $^{31}P\{^1H\}$ NMR (243 MHz, $CDCl_3$): δ 106.0 (dd, $J_{Pt\text{-}P}$ = 2678, $J_{P\text{-}P\ trans}$ = 436, $J_{P\text{-}P\ cis}$ = 21), 20.7 (dd, $J_{Pt\text{-}P}$ = 2160, $J_{P\text{-}P\ trans}$ = 436, $J_{P\text{-}P\ cis}$ = 16), 12.5 (dd, $J_{Pt\text{-}P}$ = 3820, $J_{P\text{-}P\ cis}$ = 22, $J_{P\text{-}P\ cis}$ = 16). ^1H NMR (600 MHz, $CDCl_3$): δ 7.98-7.82 (m, 9H, CH Ar), 7.80 (d, *J* = 8, 1H, CH Ar), 7.62-7.44 (m, 12H, CH Ar), 7.40-7.30 (m, 4H, CH Ar), 7.28 (d, *J* = 9, 1H, CH Ar), 7.24-7.06 (m, 6H), 4.82 (br, 1H, CH Cp), 4.76 (br, 1H, CH Cp), 4.55 (br, 1H, CH Cp), 4.53 (br, 1H, CH Cp), 4.30 (br, 1H, CH Cp), 4.24 (br, 1H, CH Cp), 3.64-3.60 (m, 2H, CH Cp), 3.50 (dd, *J* = 13, 7, 1H, CH_2), 3.29 (d, *J* = 15, 1H, CH_2), 2.84 (br m, 1H, CH_2), 2.63–2.53 (m, 1H, CH_2). The P-OH signal was not observed, but integration suggested it was obscured under the aromatic peaks. $^{13}C\{^1H\}$ NMR (151 MHz, $CDCl_3$): δ 135.6 (d, *J* = 11, CH Ar), 135.2 (d, *J* = 12, CH Ar), 135.1 (d, *J* = 5, quat Ar), 134.9 (d, *J* = 11, CH Ar), 134.6 (d, *J* = 12, CH Ar), 133.5 (d, J = 3, quat Ar), 133.2 (d, J = 2, quat Ar), 132.9 (d, J = 2, quat Ar), 132.7 (d, J = 2, Ar), 132.6 (d, *J* = 3, CH Ar), 132.1 (br, quat Ar), 131.7 (br, quat Ar), 131.6 (d, *J* = 10, quat Ar), 131.5 (d, *J* = 2, quat Ar), 131.5 (d, J = 3, CH Ar), 131.4 (d, J = 3, CH Ar), 131.0 (dd, *J* = 56, 2, quat Ar), 130.0 (d, *J* = 57, quat Ar), 129.9 (d, *J* = 4, quat Ar), 129.5 (quat Ar), 129.2 (CH Ar), 129.1 (CH Ar), 128.9-128.8 (m, CH Ar), 128.8 (CH Ar), 128.7 (CH Ar), 128.7-128.6 (m, CH Ar), 128.6 (CH Ar), 128.5 (CH Ar), 128.3 (CH Ar), 128.1 (d, *J* = 2, CH Ar), 127.4 (CH Ar), 126.7 (CH Ar), 126.4 (CH Ar), 126.0 (CH Ar), 125.9 (CH Ar), 125.5 (CH Ar), 76.8 (d, *J* = 12, CH Cp, obscured by $CDCl_3$ signal), 76.6 (d, *J* = 12, CH Cp), 75.8 (d, *J* = 10, CH Cp), 75.6 (d, *J* = 9, CH Cp), 74.8 (apparent t, *J* = 9, CH Cp), 74.5 (quat Cp, overlapping), 74.1 (d, *J* = 7, CH Cp), 73.4 (d, *J* = 7, CH Cp), 70.0 (d, *J* = 57, quat Cp), 35.9 (dd, *J* = 39, 6, CH_2), 34.7 (dd, *J* = 34, 6, CH_2). $^{19}F\{^1H\}$ NMR (565 MHz, $CDCl_3$): δ -77.9.

[Pt((*R,R*)-Me-FerroLANE)(PEt$_2$OH)][OTf]$_2$ (10) An orange CH_2Cl_2 solution of freshly prepared [Pt((*R,R*)-Me-FerroLANE)(PEt$_2$OH)(Cl)][OTf] (**2**, 56 mg, 0.062 mmol) was added to solid AgOTf (98%, 18 mg, 0.068 mmol, 1.1 equiv) to give a white precipitate. The mixture was stirred for 2 h, and the solvent was removed under vacuum. The residue was extracted with minimal CH_2Cl_2 and the resulting solution was filtered through a Celite column. The filtrate was evaporated under vacuum. The residue was washed with pentane to give an orange powder that was dried under vacuum for 1 h (55 mg, 87%).

HRMS (ESI+) m/z calcd. for $[C_{26}H_{42}FeOP_3Pt]^{2+}$ $((M–H)^+)$: 714.1446; found, 714.1475. $^{31}P\{^1H\}$ NMR (243 MHz, CD_2Cl_2): δ 112.3 (t, $J_{Pt\text{-}P}$ = 4454, $J_{P\text{-}P\ cis}$ = 11), 18.8 (d, $J_{Pt\text{-}P}$ = 2227, $J_{P\text{-}P\ cis}$ = 11). ^1H NMR (600 MHz, CD_2Cl_2): δ 10.20 (br, 1H, OH), 6.64 (2H, CH Cp), 4.94 (2H, CH Cp), 4.49 (2H, CH Cp), 4.29 (2H, CH Cp), 3.18–3.10 (m, 2H, CH), 2.94–2.87 (br, 2H, CH), 2.86–2.78 (m, 2H, CH_2 P*Et*$_2$OH), 2.44–2.33 (br, 4H, CH_2), 2.33–2.18 (m, 2H, CH_2 P*Et*$_2$OH), 1.71–1.62 (m, 2H, CH_2), 1.61–1.52 (m, 2H, CH_2), 1.50–1.41 (m, 6H, CH_3 P*Et*$_2$OH), 1.41–1.35 (m, 6H, CH_3), 1.16 (vq, *J* = 8, 6H, CH_3). $^{13}C\{^1H\}$ NMR (151 MHz, CD_2Cl_2): δ 88.2 (br, CH Cp), 80.7 (br, CH Cp), 74.0 (vt, *J* = 7, CH Cp), 66.3 (br, CH Cp), 55.8 (vt, *J* = 19, quat Cp), 36.3–35.8 (m, CH_2), 34.8–34.7 (m, CH_2), 34.6 (vt, *J* = 18, CH), 33.0 (vt, *J* = 16, CH), 30.7 (d, *J* = 5, CH_2 P*Et*$_2$OH), 30.4 (d, *J* = 6, CH_2 P*Et*$_2$OH), 19.0–18.8 (m, CH_3), 15.6 (CH_3), 9.0 (d, *J* = 4, CH_3 P*Et*$_2$OH), 8.8 (d, *J* = 4, CH_3 P*Et*$_2$OH). $^{19}F\{^1H\}$ NMR (565 MHz, CD_2Cl_2): δ –78.2.

[Pt((*R,R*)-Et-FerroLANE)(PMe$_2$OH)][OTf]$_2$ (11) Under N_2, a yellow CH_2Cl_2 solution of freshly prepared [Pt((*R,R*)-Et-FerroLANE)(PMe$_2$OH)(Cl)][OTf] (**3**, 58.8 mg, 0.063 mmol) was added to solid AgOTf (98%, 18 mg, 0.07 mmol, 1.1 equiv). A white precipitate appeared. The mixture was protected from light and stirred overnight. The solvent and volatiles were removed under vacuum. The residue was extracted with CH_2Cl_2 and the resulting solution was filtered through a Celite column. The filtrate was evaporated under vacuum. The residue was washed with pentane to give an orange powder that was dried under vacuum for 1 h (30 mg, 46%). This material was not obtained pure, but it was identified by mass spectrometry and ^1H and $^{31}P\{^1H\}$ NMR spectroscopy.

HRMS (ESI+) m/z calcd. for $[C_{28}H_{46}FeOP_3Pt]^+$ $((M–H)^+)$: 742.1759, Found: 742.1764. $^{31}P\{^1H\}$ NMR (243 MHz, CD_2Cl_2): δ 87.9 (br, $J_{Pt\text{-}P}$ = 4544), 7.3 (d, $J_{Pt\text{-}P}$ = 2194, $J_{P\text{-}P\ cis}$ = 12). ^1H NMR (600 MHz, CD_2Cl_2): δ 10.54 (br, 1H, OH), 6.65 (2H, CH Cp), 5.09 (2H, CH Cp), 4.34 (2H, CH Cp), 3.97 (2H, CH Cp), 3.10-2.85 (m, 2H), 2.78-2.66 (m, 2H), 2.55-2.35 [m, 12 H, overlaps (6H + 2.46 (d, *J* = 12, 3H, CH_3 P*Me*$_2$OH) + 2.42 (d, *J* = 12, 3H, CH_3 P*Me*$_2$OH))], 1.86-1.78 (m, 2H), 1.74-1.68 (m, 2H), 1.66-1.47 (m, 4H), 1.44-1.35 (m, 2H), 1.14-1.02 [m, 12H total, overlapping 1.09 (t, *J* = 7, 6H, Et CH_3) + 1.07 (t, *J* = 8, 6H, Et CH_3)].

[Pt((*R,R*)-*i*-Pr-FerroLANE)(PMe$_2$OH)][OTf]$_2$ (12) A yellow CH_2Cl_2 solution of [Pt((*R,R*)-*i*-Pr-FerroLANE)(PMe$_2$OH)(Cl)][OTf] (**4**, 55 mg, 0.056 mmol) was added to solid AgOTf (98%, 16.3 mg, 0.062 mmol, 1.1 equiv). The mixture was protected from light and stirred for 36 h. $^{31}P\{^1H\}$ NMR monitoring showed a 1:3 mixture of product and starting material. Fresh AgOTf (98%, 12.1 mg, 0.046 mmol) was added and the reaction mixture was stirred for 6 d. $^{31}P\{^1H\}$ NMR monitoring showed approximately 75% conversion. Fresh AgOTf (98%, 3.9 mg, 0.015 mmol) was added and the mixture was stirred at room temperature overnight. $^{31}P\{^1H\}$ NMR monitoring showed approximately 85% conversion. Fresh AgOTf was added twice more at room temperature (98%; 9 mg, 0.034 mmol, 24 h, then 5 mg, 0.019 mmol, overnight) to reach a maximum conversion >95%. The solvent and volatiles were removed under vacuum. The residue was extracted with CH_2Cl_2 and the resulting solution was filtered through a Celite column. The filtrate was evaporated under vacuum and the residue was washed with pentane to give an orange powder that was dried under vacuum for 1 h (47 mg, 76%).

HRMS (ESI+) m/z calcd. for $[C_{32}H_{54}FeOP_3Pt]^+$ $((M–H)^+)$: 798.2385, Found 798.2390. $^{31}P\{^1H\}$ NMR (243 MHz, CD_2Cl_2): δ 87.1 (br, $J_{Pt\text{-}P}$ = 4695), -6.0 (d, $J_{Pt\text{-}P}$ = 2179, *J* = 12). ^1H NMR (600 MHz, CD_2Cl_2): δ 10.80 (br, 1H, OH), 6.71 (2H, CH Cp), 5.35 (2H, CH Cp), 4.10 (2H, CH Cp), 3.54 (2H, CH Cp), 2.98-2.89 (m, 2H, CH), 2.63-2.54 (m, 2H, CH), 2.53-2.36 [m, 10H overlaps (4H, CH_2) + 2.47 (apparent t, *J* = 11, 6H, CH_3 P*Me*$_2$OH)], 1.92-1.85 (m, 2H, CH *i*-Pr), 1.82-1.73 (m, 2H, CH *i*-Pr), 1.68-1.54 (m, 4H, CH_2), 1.17 (d, *J* = 6, 6H, CH_3 *i*-Pr), 1.07 (d, *J* = 6, 12H, CH_3 *i*-Pr), 0.98 (d, *J* = 6, 6H, CH_3 *i*-Pr). $^{13}C\{^1H\}$ NMR (151 MHz, CD_2Cl_2): δ 88.9 (CH Cp), 83.3 (CH Cp), 74.7 (m, CH Cp), 69.3 (CH Cp), 52.4 (t, *J* = 17, quat Cp), 50.2 (t, *J* = 16, CH phospholane), 47.3 (t, *J* = 15, CH), 32.0 (br, CH_2), 31.6-31.4 (m, CH *i*-Pr), 28.7 (CH *i*-Pr), 26.9 (CH_3 *i*-Pr), 26.3 (d, *J* = 7, CH_3 P*Me*$_2$OH), 25.9 (d, *J* = 7, CH_3 P*Me*$_2$OH), 25.6 (CH_3 *i*-Pr), 21.5 (t, *J* = 5, CH_3 *i*-Pr), 21.3 (t, *J* = 7, CH_3 *i*-Pr). $^{19}F\{^1H\}$ NMR (565 MHz, CD_2Cl_2): δ -78.4.

[Pt((*S,S*)-Et-FerroTANE)(PMe$_2$OH)(OTf)][OTf] (13) To a yellow THF solution of Pt((*S,S*)-Et-FerroTANE)Cl_2 (50 mg, 0.071 mmol) and PMe_2OH (95%, 11.8 mg, 0.14 mmol, 2 equiv), a THF solution of

AgOTf (98%, 83 mg, 0.32 mmol, 4.5 equiv) was added dropwise. A white precipitate appeared. The mixture was stirred magnetically in an oil bath at 60 °C overnight. After cooling to room temperature, the solvent and volatile materials were removed under vacuum. The residue was extracted with minimal CH_2Cl_2 and the resulting solution was filtered through a Celite column. The filtrate was evaporated and washed with pentane to give a yellow powder, which still contained residual silver (grey precipitate appeared when it was redissolved in CH_2Cl_2). This mixture was filtered again through Celite to give a clear filtrate. Solvent was removed under reduced pressure to give an orange powder that was washed with pentane (63 mg, 88% yield, but this material still contained residual silver). According to NMR spectroscopy, this material was a mixture of a four-coordinate complex, presumably with a coordinated triflate, and unidentified impurities.

$^{31}P\{^1H\}$ NMR (243 MHz, CD_2Cl_2): δ 99.8 (dd, J_{Pt-P} = 2886, $J_{P-P\ trans}$ = 378, $J_{P-P\ cis}$ = 31), 53.2 (br d, J_{Pt-P} = 2030, $J_{P-P\ trans}$ = 380), 40.0 (br, J_{Pt-P} = 3876). On treatment with water, this complex was mostly converted to a new product, presumably [Pt((*S*,*S*)-Et-FerroTANE)(PMe_2OH)(H_2O)][OTf]$_2$, $^{31}P\{^1H\}$ NMR (243 MHz, CD_2Cl_2): δ 70.6 (d, J_{Pt-P} = 2620, $J_{P-P\ trans}$ = 365), 52.8 (br d, $J_{P-P\ trans}$ = 365), 31.7 (br, J_{Pt-P} = 3600).

[Pt(dppf)(*R*-DMB-P(OH))][OTf]$_2$ (14) Under N_2, a yellow CH_2Cl_2 solution of [Pt(dppf)(*R*-DMB-P(OH))(Cl)][OTf] (**6**, 50.2 mg, 0.039 mmol) was added to solid AgOTf (99%, 12.4 mg, 0.047 mmol, 1.2 equiv). The mixture was protected from light and stirred for 1.5 h. The solvent and volatile materials were removed under vacuum. The residue was extracted with CH_2Cl_2 and the resulting solution was filtered through a Celite column. The filtrate was evaporated under vacuum. The residue was washed with pentane to give an orange powder that was dried under vacuum for 2 h (51.7 mg, 96%). NMR spectroscopy showed that the "three-coordinate" complex was the major species present, along with unidentified impurities.

HRMS (ESI+) m/z calcd. for $[C_{56}H_{44}FeOP_3Pt]^+$ ($(M-H)^+$): 1076.1602, Found 1076.1602. $^{31}P\{^1H\}$ NMR (243 MHz, CD_2Cl_2): δ 105.7 (br, J_{Pt-P} = 4046), -12.3 (d, J_{Pt-P} = 2448, $J_{P-P\ cis}$ = 12). ^1H NMR (600 MHz, $CDCl_3$): δ 8.12-7.21 (m, 28H, CH Ar), 7.19 (t, *J* = 8, 1H, CH Ar), 7.14 (t, *J* = 8, 1H, CH Ar), 6.98 (d, *J* = 8, 1H, CH Ar), 6.92 (d, *J* = 9, 1H, CH Ar), 5.94 (br, 2H, CH Cp), 5.57 (br, 2H, CH Cp), 4.28 (2H, CH Cp), 4.20 (2H, CH Cp), 3.81-3.69 (m, 1H, CH_2), 3.17 (dd, *J* = 20, 14, 1H, CH_2), 3.10-3.02 (m, 1H, CH_2), 2.81 (d, *J* = 15, 1H, CH_2). The P-OH signal was not observed. $^{13}C\{^1H\}$ NMR (151 MHz, $CDCl_3$): δ 134.6-134.0 (m, CH Ar), 133.8 (d, *J* = 4, quat Ar), 133.6 (CH Ar), 133.5-133.1 (m, CH Ar), 132.3 (d, *J* = 2, quat Ar), 131.8 (quat Ar), 131.2 (CH Ar), 131.0-130.5 (m, CH Ar), 130.3 (quat Ar), 130.2-129.9 (m, CH Ar), 129.7-129.3 (m, CH Ar), 129.1 (d, *J* = 11, CH Ar), 128.9 (CH Ar), 128.6 (CH Ar), 128.1-127.9 (m, CH Ar), 127.6 (d, *J* = 4, CH Ar), 127.5 (d, *J* = 6, quat Ar), 126.8-126.5 (m, CH Ar), 126.3 (d, *J* = 8, CH Ar), 125.9 (CH Ar), 121.6 (t, *J* = 32, quat Ar), 120.9 (t, *J* = 33, quat Ar), 85.9 (CH Cp), 84.4 (CH Cp), 76.8 (obscured by $CDCl_3$ signals, CH Cp), 75.5 (CH Cp), 71.9 (CH Cp), 70.6 (CH Cp), 43.4 (d, *J* = 31, CH_2), 39.0 (d, *J* = 49, CH_2). The quaternary Cp signals were not observed. $^{19}F\{^1H\}$ NMR (565 MHz, CD_2Cl_2): δ -77.6.

Attempted kinetic resolution of *rac*-Keppra nitrile through partial hydration catalyzed by [Pt((*R*,*R*)-Me-FerroLANE)(PMe_2OH)][OTf]$_2$ (9) In the air, five separate $CDCl_3$ solutions of *rac*-Keppra nitrile (40 mg, 0.26 mmol) were added to separate vials loaded with solid [Pt((*R*,*R*)-Me-FerroLANE)(PMe_2OH)][OTf]$_2$ (**9**, 3 mg, 0.003 mmol, 1 mol %). The resulting yellow solutions were transferred to NMR tubes using an approximate total $CDCl_3$ volume of 0.5 mL per sample. Variable amounts of H_2O were added to each NMR tube (Table S1). The resulting heterogeneous reaction mixtures were shaken until a single phase formed (yellow solutions, ca. 15 min). Conversion was determined by ^1H NMR integration using signature signals for methyl groups in both the substrate nitrile at δ_H 0.98 (t, *J* = 9, 3H), and the product amide at δ_H 0.85 (t, *J* = 9, 3H). Each reaction mixture was chromatographed over silica gel loaded in glass Pasteur pipettes, eluting with a 97:3 v/v mixture of CH_2Cl_2/MeOH. A total of 24 fractions of about 1 mL each were collected. Nitrile eluted in fractions 1–12 (R_F ~ 0.5), while amide was collected in fractions 14–24. The combined nitrile or amide fractions were evaporated to dryness and dissolved in $CDCl_3$ for ^1H NMR analysis. The NMR samples were pumped down under vacuum to remove residual solvents and yield a pale yellow oil (nitrile) or a colorless to off-white solid (amide). Each sample was dissolved with up to 30 drops of HPLC grade isopropanol (IPA), and enough HPLC grade hexanes were added to result in a volume of about 1.5 mL. If some cloudiness was observed, the mixtures were filtered through Celite to give clear colorless solutions. Chiral HPLC analysis of these solutions was performed for both compounds (for nitrile: Chiralcel OD-H, Hexane/IPA = 90:10, 1 mL min^{-1}, 225 nm, τ_R 14.373 min, τ_S 20.314 min; for amide: Chiralpak AD-H, Hexane/IPA = 85:15, 1 mL min^{-1}, 225 nm, τ_R 8.070 min, τ_S 11.316 min). Enantiomeric ratios (*e.r.*) were obtained by integration of the chromatograms. Catalytic hydration of *rac*-Keppra nitrile under kinetic resolution conditions with other precursors was carried out similarly (see the SI).

Reaction of [Pt((*R*,*R*)-Me-FerroLANE)(PMe_2OH)][OTf]$_2$ (9) with *S*-Keppra nitrile gave the metallacycle [Pt((*R*,*R*)-Me-FerroLANE)($PMe_2OC(R^*)$=NH)][OTf]$_2$ (*S*-15, R* = *S*-CH(Et)(*cyclo*-$N(CH_2)_3C(O)$-) A CD_2Cl_2 solution of (*S*)-Keppra-nitrile (14.1 mg, 0.093 mmol, 3.1 equiv) was added to solid [Pt((*R*,*R*)-Me-FerroLANE)(PMe_2OH)][OTf]$_2$ (**9**, 30 mg, 0.030 mmol) to give a yellow solution. NMR analysis showed selective formation of a single Pt product. Attempts to isolate this product after removal of the solvent under vacuum and washing the residue with pentane, or by recrystallization, were unsuccessful, yielding precursor dication **9**, or (see below) the iminol complex *S*-**25** formed in catalytic nitrile hydration with residual water in the solvent. The mixture of excess nitrile and metallacycle was characterized by multinuclear NMR spectroscopy.

$^{31}P\{^1H\}$ NMR (243 MHz, CD_2Cl_2): δ 164.9 (dd, J_{Pt-P} = 2412, $J_{P-P(trans)}$ = 355, $J_{P-P(cis)}$ = 21), 37.8 (dd, J_{Pt-P} = 2435, $J_{P-P(trans)}$ = 355, $J_{P-P(cis)}$ = 13), 25.0 (d, J_{Pt-P} = 3159, $J_{P-P(cis)}$ = 21, $J_{P-P(cis)}$ = 13).

^1H NMR (600 MHz, CD_2Cl_2): δ 9.58 (1H, NH), 5.02–4.93 (m, overlaps CH + CH $_{nitrile}$), 4.86 (br, 2H, CH Cp), 4.65 (br, 2H, CH Cp), 4.55 (br, 1H, CH Cp), 4.46 (br, 2H, CH Cp), 4.40 (br, 1H, CH Cp), 3.71–3.58 (m, 2H, CH_2), 3.16–3.02 (m, 2H, CH), 2.96–2.87 (m, 1H, CH), 2.60–2.34 (m, overlaps PMe_2O [2.54 (d, *J* = 7, 3H)] + PMe_2O [2.43 (d, *J* = 7, 3H)] + CH_2 (2H) + CH_2 $_{nitrile}$), 2.33–2.23 (m, 3H, CH + CH_2), 2.18–2.02 (overlaps CH_2 (2H) + CH_2 $_{nitrile}$), 1.97–1.88 (m, overlaps CH_2 (1H) + CH_2 $_{nitrile}$), 1.84–1.65 (m, overlaps CH_2 (1H) + CH_2 $_{nitrile}$ + CH_3 phospholane [1.71 (dd, *J* = 21, 7, 3H)] + CH_2 phospholane [1H]), 1.61–1.50 (m, overlaps CH_3 phospholane [1.57 (dd, *J* = 20, 7, 3H)] + CH_2 phospholane [1H]), 1.48–1.37 (m, 2H, CH_2), 1.13 (dd, *J* = 17, 7, 3H, CH_3), 1.05–0.97 (m, overlaps CH_3 (3H) + CH_3 $_{nitrile}$), 0.94 (dd, *J* = 17, 6, 3H, CH_3). Signals for unreacted starting *S*-Keppra-nitrile: δ 4.98 (t, *J* = 8, 1H), 3.50–3.37 (m, 2H), 2.41–2.36 (m, 2H), 2.16–2.01 (m, 2H), 1.96–1.86 (m, 1H), 1.83–1.75 (m, 1H), 1.00 (t, *J* = 7, 3H).

$^{13}C\{^1H\}$ NMR (151 MHz, CD_2Cl_2): δ 182.6 (quat C), 178.9 (quat C), 121.1 (br q, J = 320, CF_3), 77.7 (d, *J* = 9, CH Cp), 77.5 (d, *J* = 10, CH Cp), 76.9 (d, *J* = 14, CH Cp), 76.1 (d, *J* = 5, CH Cp), 75.3 (d, *J* = 6, CH Cp), 75.2–75.0 (br, CH Cp), 74.9 (d, *J* = 6, CH Cp), 74.1 (d, *J* = 13, CH Cp), 65.4 (dd, *J* = 63, 6, quat Cp), 59.7 (d, *J* = 55, quat Cp), 56.5 (CH), 48.0 (CH_2), 43.0 (dd, *J* = 41, 9, CH phospholane), 38.9 (dd, *J* = 29, 3, CH phospholane), 37.6 (d, *J* = 41, CH phospholane), 36.8 (d, *J* = 33, CH phospholane), 36.6 (d, *J* = 4, CH_2 phospholane), 36.3 (br, CH_2 phospholane), 35.8 (br, CH_2 phospholane), 35.5 (br, CH_2 phospholane), 31.6 (CH_2), 23.4 (CH_2), 22.1 (d, *J* = 5, CH_3), 20.6 (d, *J* = 6, CH_3), 19.8 (dd, *J* = 32, 5, P*Me*$_2$O), 19.2–18.8 [m, overlaps *C*H$_2$ (19.1) + P*Me*$_2$O (18.9, dd, *J* = 32, 5)], 14.6 (CH_3 phospholane), 13.9 (CH_3 phospholane), 10.7 (CH_3). Signals for unreacted starting Keppra nitrile: δ 174.9 (C=O), 117.5 (C≡N), 44.4 (CH), 43.7 (CH_2), 30.6 (CH_2), 25.0 (CH_2), 18.1 (CH_2), 10.2 (CH_3).

$^{19}F\{^1H\}$ NMR (565 MHz, CD_2Cl_2): δ -78.3 (OTf^-). ^{15}N NMR via ^{15}N-^1H HSQC (^1H 700 MHz, ^{15}N 71 MHz; CD_2Cl_2): δ 171.4 (d, J_{Pt-N} = 244, $J_{P-N(trans)}$ = 38, J_{H-N} = 77).

Reaction of [Pt((*R*,*R*)-Me-FerroLANE)(PMe_2OH)][OTf]$_2$ (9) with racemic Keppra nitrile and diastereoselective formation of the metallacycles [Pt((*R*,*R*)-Me-FerroLANE)($PMe_2OC(R^*)$=NH)][OTf]$_2$ (15, R* = *R*/*S*-CH(Et)(*cyclo*-$N(CH_2)_3C(O)$-) A CD_2Cl_2 solution of *rac*-Keppra-nitrile (18.5 mg, 0.122 mmol, 3 equiv) was added to solid [Pt((*R*,*R*)-Me-FerroLANE)(PMe_2OH)][OTf]$_2$ (**9**, 40 mg, 0.041 mmol) to give a yellow

solution of a 1.7:1 mixture of diastereomers A (major, from the *R*-nitrile) and B (minor, from the *S*-nitrile, see above). Attempted isolation was unsuccessful, so the mixture of diastereomers, unreacted nitrile, and amide formed by hydration with residual water, was characterized by NMR spectroscopy. The ^{31}P, ^{15}N, and ^{13}C NMR signals for the major diastereomer were mostly distinct from those of the minor diastereomer, so they are reported separately below, but the ^{1}H NMR spectrum contained extensive overlap. The ^{19}F NMR spectrum (triflate anion) was the same for both isomers.

^{31}P{^{1}H} NMR (243 MHz, CD_2Cl_2): δ 163.6 (dd, J_{Pt-P} = 2422, $J_{P-P\ trans}$ = 355, $J_{P-P\ cis}$ = 21), 38.3 (dd, J_{Pt-P} = 2442, $J_{P-P\ trans}$ = 355, $J_{P-P\ cis}$ = 14), 24.8 (dd, J_{Pt-P} = 3144, $J_{P-P\ cis}$ = 21, $J_{P-P\ cis}$ = 14).

^{1}H NMR (600 MHz, CD_2Cl_2): δ 10.36 (1H, NH B), 9.73 (1H, NH A), 6.26 (1H, $NH_{2\ amide}$), 5.57 (1H, $NH_{2\ amide}$), 4.95 (t, *J* = 8, 1H, $CH_{nitrile}$), 4.87–4.85 (m, CH Cp A + B), 4.71–4.67 (m, 1H, CH A), 4.65 (br, CH Cp (A + B) + CH B), 4.55 (br, CH Cp A + B), 4.48 (br, CH Cp A + B), 4.45 (br, CH Cp A + B), 4.40 (br, CH Cp (A + B) + CH_{amide}), 3.83–3.77 (m, 1H, CH_2 B), 3.71–3.66 (m, 1H, CH_2 A), 3.62–3.55 (m, 1H, CH_2 A), 3.51–3.32 (m, overlaps CH_2 B + $CH_{2\ nitrile}$ + $CH_{2\ amide}$), 3.14–3.02 (m, overlaps CH phospholane (A + B) + CH_2 phospholane (A + B)), 2.93–2.83 (m, overlaps CH phospholane (A + B)), 2.61–2.32 (m, overlaps PMe_2O B [2.57 (d, *J* = 9, 3H)] + PMe_2O A [2.53 (d, *J* = 9, 3H)] + PMe_2O (2.43 (d, *J* = 9, 3H)] + CH phospholane (A + B) + CH_2 phospholane (A + B) + $CH_{2\ nitrile}$ [2.36 (apparent t, *J* = 9, 2H)] + $CH_{2\ amide}$), 2.31–2.17 (m, overlaps CH phospholane (A + B) + CH_2 phospholane (A + B)), 2.16–1.97 (m, overlaps $CH_{2\ nitrile}$ + $CH_{2\ amide}$), 1.96–1.85 (m, overlaps $CH_{2\ nitrile}$ + $CH_{2\ amide}$ + CH_2 phospholane (A + B)), 1.84–1.63 (m, overlaps CH_2 nitrile + $CH_{2\ amide}$ + CH_2 phospholane (A + B) + CH_3 phospholane (A + B), 6H), 1.61–1.50 (m, overlaps CH_2 phospholane (A + B) + CH_3 phospholane A [1.58 (dd, *J* = 20, 8, 3H)] + CH_3 phospholane B [1.56 (dd, *J* = 20, 7, 3H)]), 1.49–1.35 (m + CH_2 phospholane (A + B)), 1.15–1.07 (m, overlaps CH_3 phospholane (A+B), 6H), 1.05–0.97 (m, overlaps CH_3 phospholane B (3H) + CH_3 A (3H) + $CH_{3\ nitrile}$), 0.94 (dd, *J* = 17, 6, 3H, CH_3 phospholane A), 0.87 (apparent t, *J* = 7, overlaps CH_3 A (3H) + $CH_{3\ amide}$). Signals for Keppra-amide: ^{1}H NMR (CD_2Cl_2): δ 6.33 (br, 1H, NH), 5.66 (br, 1H, NH), 4.43 (dd, J = 9, 6, CH), 3.41-3.34 (m, 2H, CH_2), 2.42-2.31 (m, 2H, CH_2), 2.04-1.98 (m, 2H, CH_2), 1.96-1.88 (m, 1H, CH_2), 1.70-1.63 (m, 1H, CH_2), 0.88 (t, J = 7, Me).

^{13}C{^{1}H} NMR (151 MHz, CD_2Cl_2): δ 182.4–182.2 (m, quat C=NH), 178.6 (quat C=O), 77.6 (d, *J* = 9, CH Cp), 77.4 (d, *J* = 10, CH Cp), 76.8 (d, *J* = 14, CH Cp), 76.0 (d, *J* = 5, CH Cp), 75.3 (apparent t, *J* = 6, overlaps CH Cp A + CH Cp B), 75.2–75.0 (m, overlaps CH Cp A + CH Cp B), 74.9–74.7 (m, overlaps CH Cp A + CH Cp B), 74.0 (d, *J* = 14, overlaps CH Cp A + CH Cp B), 65.5 (dd, J_{C-P} = 63, *J* = 5, quat Cp), 59.9 (d, J_{C-P} = 55, quat Cp), 57.6 (br, CH), 49.3 (CH_2), 42.9 (dd, *J* = 41, 9, CH phospholane), 39.0 (dd, *J* = 29, 3, CH phospholane), 37.6 (d, *J* = 42, CH phospholane), 36.5 (d, *J* = 33, CH phospholane), 36.7 (apparent d, *J* = 4, CH_2 phospholane), 35.9–35.7 (m, overlaps CH_2 phospholane A + CH_2 phospholane B), 35.6 (br, overlaps CH_2 phospholane A + CH_2 phospholane B), 31.8 (CH_2), 23.4 (CH_2), 22.1 (d, *J* = 5, CH_3 phospholane), 20.6–20.3 [m, overlaps CH_3 phospholane A (20.5 (d, *J* = 4)) + CH_3 phospholane B [20.4 (d, *J* = 5))], 19.6 (dd, *J* = 32, 5, PMe_2O), 19.3–18.7 [m, overlaps PMe_2O B [19.1 (dd, *J* = 28, 5)] + CH_2 A (19.1) + CH_2 B (18.9) + PMe_2O A [18.9 (dd, *J* = 33, 5)]], 14.5 (CH_3 phospholane), 13.9 (CH_3 phospholane), 10.8 (CH_3). Signals for Keppra-amide (see above for nitrile peaks): δ 176.2 (quat *C*), 172.5 (quat *C*), 56.6 (*C*H), 44.2 (CH_2), 31.4 (CH_2), 21.42 (CH_2), 18.5 (CH_2), 10.7 (CH_3). ^{19}F{^{1}H} NMR (565 MHz, CD_2Cl_2): δ -78.7 (OTf^-). ^{15}N NMR via ^{15}N-^{1}H HSQC (^{1}H 700 MHz, ^{15}N 71 MHz; CD_2Cl_2) δ 173.7 (d, J_{Pt-N} = 240, $J_{P-N\ trans}$ = 38, J_{H-N} = 77).

Diastereoselective generation of metallacycles 16-19 from cationic [Pt(diphos*)(SPO)]$^{2+}$ complexes and excess racemic Keppra nitrile To the solid Pt complexes [(a) [Pt((*R*,*R*)-Me-FerroLANE)(PMe_2OH)][$OTf]_2$ (**9**, 40 mg, 0.041 mmol), (b) [Pt((*R*,*R*)-Et-FerroLANE)(PMe_2OH)][$OTf]_2$ (**11**, 30 mg, 0.029 mmol), (c) [Pt((*R*,*R*)-*i*-Pr-FerroLANE)(PMe_2OH)][$OTf]_2$ (**12**, 16 mg, 0.014 mmol), (d) [Pt((*R*,*R*)-Me-FerroLANE)(PEt_2OH)][$OTf]_2$ (**10**, 15 mg, 0.015 mmol), (e) [Pt((*S*,*S*)-Et-FerroTANE)(PMe_2OH)(OTf)][OTf] (**13**, 21 mg, 0.021 mmol), (f) [Pt(dppf)(R-DMB-P(OH))][$OTf]_2$ (**14**, 16.7 mg, 0.12 mmol)] were added CD_2Cl_2 solutions of racemic Keppra nitrile [(a) 19.7 mg, 0.13 mmol, 3.2 equiv; (b) 13.6 mg, 0.089 mmol, 3.1 equiv; (c) 6.5 mg, 0.043 mmol, 3.1 equiv; (d) 7 mg, 0.046 mmol, 3.1 equiv; (e) 9.5 mg, 0.062 mmol, 3 equiv; (f) 7.3 mg, 0.048 mmol, 4 equiv; $CDCl_3$ was used instead of CD_2Cl_2]. The mixtures (a–e) were transferred to screw cap NMR tubes for analysis. Except for mixture (c), which was deep orange, all reaction mixtures a-e formed yellow solutions. Sample (f), which formed a clear orange solution, was prepared and analyzed in a standard NMR tube, opened to air. ^{31}P{^{1}H} and ^{1}H NMR spectra were recorded at room temperature, at least 24 h after sample preparation. The dr values (see Table 1 and the SI) were determined by ^{31}P{^{1}H} NMR integration.

Diastereoselective generation of metallacycles 15 and 20-24 from [Pt((*R*,*R*)-Me-FerroLANE)(PMe_2OH)][$OTf]_2$ (9) and the racemic nitriles PhCH(R)(CN) (R = Me, Et, *i*-Pr, Cy), cyclopropane-nitrile $Ph_2CCH_2CH(CN)$, or *rac*-Keppra nitrile CD_2Cl_2 solutions of the nitriles PhCH(R)(CN) [(a) R = Me (8 mg, 0.061 mmol), (b) R = Et (8.9 mg, 0.061 mmol), (c) R = *i*-Pr (9.7 mg, 0.061 mmol), (d) R = Cy (12.2 mg, 0.061 mmol), (e) cyclopropane-nitrile (15 mg, 0.068 mmol) (f) *rac*-Keppra-nitrile (19.7 mg, 0.13 mmol)] were added to solid [Pt((*R*,*R*)-Me-FerroLANE)(PMe_2OH)][$OTf]_2$ [(a–d) 20 mg, 0.02 mmol; (e) 6 mg, 0.006 mmol; (f) 40 mg, 0.041 mmol]. All mixtures were prepared with a 3:1 nitrile to Pt complex ratio, except for (e), which was 10:1. The resulting yellow solutions were transferred to screw cap NMR tubes. ^{31}P{^{1}H} and ^{1}H NMR spectra were recorded 24 h after sample preparation. Diastereomeric ratio (*dr*) values were determined by ^{31}P{^{1}H} NMR integration.

Generation of the Iminol Complexes [Pt((*R*,*R*)-Me-FerroLANE)(PMe_2OH)(NH=C(R*)(OH))][$OTf]_2$ (25, R* = CH(Et)(*cyclo*-$N(CH_2)_3C(O)$-) from Metallacycle 15 and Water, Including Labeling Studies with $^{18}OH_2$ The iminol complexes **25** were observed in several experiments in the reaction of metallacycle **15** (generated from racemic or S-Keppra nitrile and **9**) with residual water in the NMR solvents, or with deliberately added $^{16}OH_2$, $^{16}OD_2$, or $^{18}OH_2$. See the SI for details. In an example procedure, a CD_2Cl_2 solution (1 mL) of *S*-Keppra nitrile (14 mg, 0.092 mmol, 3.1 equiv) was added to solid [Pt((*R*,*R*)-Me-FerroLANE)(PMe_2OH)][$OTf]_2$ (**9**, 30 mg, 0.030 mmol). Immediate formation of a yellow solution was observed. The mixture was loaded in a screw cap NMR tube for analysis. After 15 min, ^{31}P{^{1}H} NMR analysis showed complete conversion of precursor **9** into metallacycle *S*-**15**. ^{18}O-labelled water was added (0.6 μL, 0.03 mmol, 1 equiv) and the NMR tube was shaken until a homogeneous mixture was observed again (ca. 1 min). After 15 min, ^{31}P{^{1}H} NMR analysis showed major signals for intermediate iminol complex *S*-**25**.

Generation of the Iminol Complex [Pt((*R*,*R*)-Me-FerroLANE)(PMe_2OH)(*S*-NH=C(R*)(OH))][$OTf]_2$ (*S*-25, R* = *S*-CH(Et)(*cyclo*-$N(CH_2)_3C(O)$-) from Precursor 9 and the *S*-Keppra Amide Under N_2, a solution of the Keppra amide (56.9 mg, 0.334 mmol, 11 equiv) in CD_2Cl_2 (0.7 mL) was dried overnight over molecular sieves, then added dropwise to dication **9** (30 mg, 0.0304 mmol). The resulting orange solution was transferred into a screw-cap NMR tube; the ^{31}P{^{1}H} NMR spectrum showed a 2.4:1 mixture of *S*-**25** and **9**. For *S*-**25**, ^{31}P{^{1}H} NMR (243 MHz, CD_2Cl_2): δ 88.6 (d, $J_{P-P\ trans}$ = 415, J_{Pt-P} = 2790), 35.5 (d, $J_{P-P\ trans}$ = 415, J_{Pt-P} = 2108), 22.4 (J_{Pt-P} = 3200). For **9**, ^{31}P{^{1}H} NMR (202 MHz, CD_2Cl_2): δ 19.1 (d, $J_{P-P\ cis}$ = 12, J_{Pt-P} = 2276). The 2nd peak overlapped the signal for **25** at 88.6 ppm. Selected ^{1}H NMR (600 MHz, CD_2Cl_2): δ 15.02 (1H, COH), 10.28 (1H, POH), 9.09 (1H, NH).

Generation of the aquo complex [Pt((*R*,*R*)-Me-FerroLANE)(PMe_2OH)(H_2O)][$OTf]_2$ (26) Under N_2, water (1.3 μL, 0.074 mmol, 3.0 equiv) was added to a solution of dication **9** (24.3 mg, 0.0247 mmol) in CH_2Cl_2 (0.7 mL) in a NMR tube. The tube was inverted and mixed before monitoring by ^{31}P{^{1}H} NMR spectroscopy, which showed a 2.7:1 mixture of aquo complex **26** and **9**.

For **26**, ^{31}P{^{1}H} NMR (202 MHz, CD_2Cl_2): δ 97.2 (d, $J_{P-P\ trans}$ = 418, J_{Pt-P} = 2781), 46.2 (d, $J_{P-P\ trans}$ = 418, J_{Pt-P} = 2150), 32.8 (d, $J_{P-P\ cis}$ = 25, J_{Pt-P} = 3933). For **9**, ^{31}P{^{1}H} NMR (202 MHz, CD_2Cl_2): δ 88.7 (J_{Pt-P} = 4484), 20.9 (d, $J_{P-P\ cis}$ = 12, J_{Pt-P} = 2236). For the mixture of **9** and **26**, most ^{1}H NMR signals could be assigned, but some, especially for the phospholane CH_2/CH peaks, were overlapping. ^{1}H NMR (500 MHz, CD_2Cl_2): δ 6.52 (2H, Cp **9**), 4.84 (2H, Cp **9**), 4.74 (1H, Cp **26**), 4.69 (1H, Cp **26**), 4.52

(2H, Cp **26**), 4.45 (1H, Cp **26**), 4.35-4.33 (2H, Cp **9**), 4.29 (3H, Cp **26**), 3.61 (2H **26**), 3.12 (2H **9**), 2.97–2.65 (br m, **9**+**26**), 2.51-2.19 (m, PMe **9** + phospholane **26**), 2.07-1.85 (m, 6H, PMe **26**), 1.75 (2H, H_2O), 1.69-1.64 (2 overlapping dd, 6H, Me **26**), 1.44-1.17 (m, 3H, Me **9**), 1.17-1.05 (m, 3H, Me **9**), 0.98 (dd, J = 16, 7, 3H, Me **26**), 0.76 (dd, J = 18, 7, 3H, Me **26**). The P-OH signals were not observed.

When D_2O was used instead of H_2O, [**Pt((*R,R*)-Me-FerroLANE)(PMe$_2$OH)(D$_2$O)**][**OTf**]$_2$ (**26-D**) was formed: $^{31}P\{^1H\}$ NMR (243 MHz, CD_2Cl_2): δ 96.6 (d, $J_{P\text{-}P\ trans}$ = 416, $J_{Pt\text{-}P}$ = 2806), 46.0 (d, $J_{P\text{-}P\ trans}$ = 423, $J_{Pt\text{-}P}$ = 2143), 32.7 (dd, $J_{P\text{-}P\ cis}$ = 27, 10, $J_{Pt\text{-}P}$ = 3924).

ASSOCIATED CONTENT

Supporting Information

The Supporting Information is available free of charge on the ACS Publications website.

Additional details of synthesis and characterization, including NMR spectra, crystal structure information, and DFT calculations (PDF)

Computed structures (xyz)

X-ray crystallography details (CIF)

AUTHOR INFORMATION

Corresponding Author

* glueck@dartmouth.edu

The authors declare no competing financial interests.

ACKNOWLEDGMENT

We thank the American Chemical Society Petroleum Research Fund (60035-ND3) and the National Science Foundation (CHE-1954412) for support, and Maria Pellegrini for the ^{15}N-^1H HSQC NMR experiment.

REFERENCES

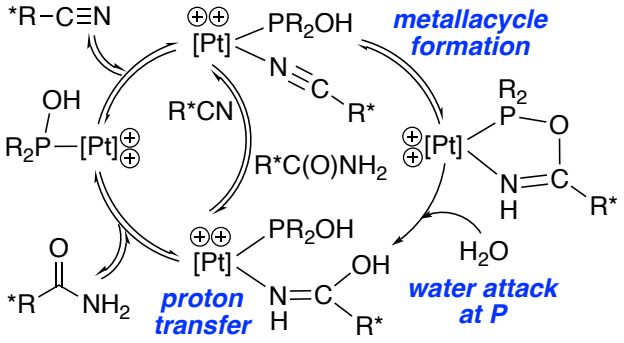

1. (a) Roughley, S. D.; Jordan, A. M. The Medicinal Chemist's Toolbox: An Analysis of Reactions Used in the Pursuit of Drug Candidates. *J. Med. Chem.* **2011**, *54*, 3451-3479. (b) Valeur, E.; Bradley, M. Amide bond formation: beyond the myth of coupling reagents. *Chem. Soc. Rev.* **2009**, *38*, 606-631.

2. (a) Glueck, D. S. Intramolecular Attack on Coordinated Nitriles: Metallacycle Intermediates in Catalytic Hydration and Beyond. *Dalton Trans*. **2021**, *50*, 15953-15960. (b) Xia, Y.; He, D.; Wu, W. Recent Advances for Hydration Reaction of Nitriles in Different Catalytic Systems. *Chin. J. Org. Chem*. **2021**, *41*, 969-982.
3. Cheng, Z.; Xia, Y.; Zhou, Z. Recent Advances and Promises in Nitrile Hydratase: From Mechanism to Industrial Applications. *Frontiers in Bioengineering and Biotechnology* **2020**, *8*, 1-18.
4. (a) Li, B.; Su, J.; Tao, J. Enzyme and Process Development for Production of Nicotinamide. *Org. Proc. Res. Dev*. **2011**, *15*, 291-293. (b) Sanchez, S.; Demain, A. L. Enzymes and Bioconversions of Industrial, Pharmaceutical, and Biotechnological Significance. *Org. Proc. Res. Dev*. **2011**, *15*, 224-230. (c) Shapiro, R.; DiCosimo, R.; Hennessey, S. M.; Stieglitz, B.; Campopiano, O.; Chiang, G. C. Discovery and Development of a Commercial Synthesis of Azafenidin. *Org. Proc. Res. Dev*. **2001**, *5*, 593-598.
5. (a) Tao, J.; Liu, J.; Chen, Z., Some Recent Examples in Developing Biocatalytic Pharmaceutical Processes. In *Asymmetric Catalysis on Industrial Scale*, Wiley-VCH Verlag GmbH & Co. KGaA: 2010; pp 1-12. (b) Tucker, J. L.; Xu, L.; Yu, W.; Scott, R. W.; Zhao, L.; Ran, N. Chemoenzymatic processes for preparation of levetiracetam. WO2009009117 (Bioverdant), 2009.
6. Gulyas, H.; Rivilla, I.; Curreli, S.; Freixa, Z.; van Leeuwen, P. W. N. M. Highly active, chemo- and enantioselective Pt-SPO catalytic systems for the synthesis of aromatic carboxamides. *Catal. Sci. Technol*. **2015**, *5*, 3822-3828.
7. Constable, D. J. C.; Dunn, P. J.; Hayler, J. D.; Humphrey, G. R.; Leazer, Jr., J. L.; Linderman, R. J.; Lorenz, K.; Manley, J.; Pearlman, B. A.; Wells, A.; Zaks, A.; Zhang, T. Y. Key green chemistry research areas—a perspective from pharmaceutical manufacturers. *Green Chem*. **2007**, *9*, 411-420.
8. (a) Cadierno, V. Synthetic Applications of the Parkins Nitrile Hydration Catalyst [PtH{$(PMe_2O)_2H$}(PMe_2OH)]: A Review. *Applied Sciences* **2015**, *5*, 380-401. (b) Xing, X.; Xu, C.; Chen, B.; Li, C.; Virgil, S. C.; Grubbs, R. H. Highly Active Platinum Catalysts for Nitrile and Cyanohydrin Hydration: Catalyst Design and Ligand Screening via High-Throughput Techniques. *J. Am. Chem. Soc*. **2018**, *140*, 17782-17789.
9. Gallen, A.; Riera, A.; Verdaguer, X.; Grabulosa, A. Coordination chemistry and catalysis with secondary phosphine oxides. *Catal. Sci. Technol*. **2019**, *9*, 5504-5561.
10. (a) Ghaffar, T.; Parkins, A. W. A New Homogeneous Platinum Containing Catalyst for the Hydrolysis of Nitriles. *Tetrahedron Lett*. **1995**, *36*, 8657-8660. (b) Parkins, A. W. Catalytic Hydration of Nitriles to Amides. *Platinum Met. Rev*. **1996**, *40*, 169-174. (c) Ghaffar, T.; Parkins, A. W. The Catalytic Hydration of Nitriles to Amides Using a Homogeneous Platinum Phosphinito Catalyst. *J. Molec. Catal. A: Chem*. **2000**, *160*, 249-261.
11. Li, C.; Chang, X.-Y.; Huo, L.; Tan, H.; Xing, X.; Xu, C. Hydration of Cyanohydrins by Highly Active Cationic Pt Catalysts: Mechanism and Scope. *ACS Catal*. **2021**, *11*, 8716-8726.
12. (a) Kodama, K.; Shimomura, Y.; Hirose, T. Enantiomer Separation of Nitriles and Epoxides by Crystallization with Chiral Organic Salts: Chirality Switching Modulated by Achiral Acids. *Cryst. Growth Des*. **2021**, *21*, 6552–6557. (b) Qin, L.-F.; Pang, C.-Y.; Han, W.-K.; Zhang, F.-L.; Tian, L.; Gu, Z.-G.; Ren, X.; Li, Z. Optical recognition of alkyl nitrile by a homochiral iron(II) spin crossover host. *CrystEngComm* **2015**, *17*, 7956-7963. (c) Hameed, S.; Ahmad, R.; Duddeck, H. Chiral recognition of nitriles by ^{1}H NMR spectroscopy in the presence of a chiral dirhodium complex. *Magn. Reson. Chem*. **1998**, *36*, S47-S53. (d) Rozwadowski, Z.; Malik, S.; Toth, G.; Gati, T.; Duddeck, H. Dirhodium tetraacylate complexes and monovalent ligands. Adduct formation in solution as monitored by NMR spectroscopy. *Dalton Trans*. **2003**, 375-379. (e) Schwenninger, R.; Schlögl, J.; Maynollo, J.; Gruber, K.; Ochsenbein, P.; Bürgi, H.-B.; Konrat, R.; Kräutler, B. Metal Complexes of a Biconcave Porphyrin with D_4-Structure—Versatile Chiral Shift Agents. *Chem. Eur. J*. **2001**, *7*, 2676-2686.
13. Burk, M. J.; Gross, M. F. New Chiral 1,1'-Bis(phospholano)ferrocene Ligands for Asymmetric Catalysis. *Tetrahedron Lett*. **1994**, *35*, 9363-9366.
14. Mandell, C. L.; Kleinbach, S. S.; Dougherty, W. G.; Kassel, W. S.; Nataro, C. Electrochemistry of 1,1,'-Bis(2,4-dialkylphosphetanyl)ferrocene and 1,1'-Bis(2,5-dialkylphospholanyl)ferrocene Ligands: Free Phosphines, Metal Complexes, and Chalcogenides. *Inorg. Chem*. **2010**, *49*, 9718–9727.
15. Garduño, J. A.; Glueck, D. S.; Hernandez, R. E.; Figueroa, J. S.; Rheingold, A. L. Protonolysis of the $[B(Ar_F)_4]^-$ Anion Mediated by Nucleophile/Electrophile/Water Cooperativity in a Platinum–PMe_2OH Complex. *Organometallics* **2022**, *41*, 1475-1479.
16. Berry, D. E.; Beveridge, K. A.; Bushnell, G. W.; Dixon, K. R. Hydrolysis of chlorophosphine ligands on platinum and palladium. ^{31}P and ^{195}Pt nmr studies and the crystal and molecular structures of cis-$[PtCl_2(PPh_2OH)_2]\bullet C_4H_8O$ and $[Pd_2(\mu\text{-}Cl)_2\{(P(OEt)_2O)_2H\}_2]$. *Can. J. Chem*. **1985**, *63*, 2949-2957.
17. (a) Ringenberg, M. R. Beyond Common Metal–Metal Bonds, $\varkappa^3$-Bis(donor)ferrocenyl→Transition-Metal Interactions. *Chem. – Eur. J*. **2019**, *25*, 2396-2406. (b) Oberhauser, W. Monophosphite coordination and hydrolysis by Pt(II) bearing 1,1′-bis(di(o-methoxyphenyl)phosphanyl)ferrocene. *Inorg. Chim. Acta* **2020**, *511*, 119844. (c) Cabrera, K. D.; Rowland, A. T.; Szarko, J. M.; Diaconescu, P. L.; Bezpalko, M. W.; Kassel, W. S.; Nataro, C. Monodentate phosphine substitution in $[Pd(\varkappa^3\text{-}dppf)(PR_3)][BF_4]_2$ (dppf = 1,1′-bis(diphenylphosphino)ferrocene) compounds. *Dalton Trans*. **2017**, *46*, 5702-5710. (d) Sato, M.; Shigeta, H.; Sekino, M.; Akabori, S. Synthesis, some reactions, and molecular structure of the $Pd(BF_4)_2$ complex of 1,1′-bis(diphenylphosphino)ferrocene. *J. Organomet. Chem*. **1993**, *458*, 199-204.
18. Guino-o, M. A.; Zureick, A. H.; Blank, N. F.; Anderson, B. J.; Chapp, T. W.; Kim, Y.; Glueck, D. S.; Rheingold, A. L. Synthesis and Structure of Platinum Bis(phospholane) Complexes Pt(diphos*)(R)(X), Catalyst Precursors for Asymmetric Phosphine Alkylation. *Organometallics* **2012**, *31*, 6900-6910.

19. Kenda, B. M.; Matagne, A. C.; Talaga, P. E.; Pasau, P. M.; Differding, E.; Lallemand, B. I.; Frycia, A. M.; Moureau, F. G.; Klitgaard, H. V.; Gillard, M. R.; Fuks, B.; Michel, P. Discovery of 4-Substituted Pyrrolidone Butanamides as New Agents with Significant Antiepileptic Activity. *J. Med. Chem.* **2004**, *47*, 530-549.
20. (a) Geldbach, T. J.; Drago, D.; Pregosin, P. S. A weak η^1 π-bonding mode for Ru–arene complexes. Nitrile, isonitrile and phosphine derivatives of Ru–phosphino–arene chelating complexes. *J. Organomet. Chem.* **2002**, *643–644*, 214-222. (b) Tomas-Mendivil, E.; Menendez-Rodriguez, L.; Francos, J.; Crochet, P.; Cadierno, V. Investigation of binap-based hydroxyphosphine arene-ruthenium(II) complexes as catalysts for nitrile hydration. *RSC Adv.* **2014**, *4*, 63466-63474. (c) Tomás-Mendivil, E.; Cadierno, V.; Menéndez, M. I.; López, R. Unmasking the Action of Phosphinous Acid Ligands in Nitrile Hydration Reactions Catalyzed by Arene–Ruthenium(II) Complexes. *Chem. Eur. J.* **2015**, *21*, 16874-16886.
21. Garrou, P. E. Δ_R Ring Contributions to ^{31}P NMR Parameters of Transition-Metal-Phosphorus Chelate Complexes. *Chem. Rev.* **1981**, *81*, 229-266.
22. Appleton, T. G.; Clark, H. C.; Manzer, L. E. The *trans*-influence: its measurement and significance. *Coord. Chem. Rev.* **1973**, *10*, 335-422.
23. For use of this experiment in a related Ru complex, see ref 20a. See also Lee, J. C., Jr.; Mueller, B.; Pregosin, P.; Yap, G. P. A.; Rheingold, A. L.; Crabtree, R. H. An Unusual Coordination Mode for Amides: Lone-Pair Binding via Nitrogen. *Inorg. Chem.* **1995**, *34*, 6295-6301.
24. (a) Brown, D. B.; Robin, M. B.; Burbank, R. D. Amide tautomerism. Evidence for the iminol form of trimethylacetamide in a platinum complex. *J. Am. Chem. Soc.* **1968**, *90*, 5621-5622. (b) Cini, R.; Fanizzi, F. P.; Intini, F. P.; Natile, G.; Pacifico, C. Isomerism of amides coordinated to platinum. X-ray crystal structure of dichloro-bisacetamide-platinum(II). *Inorg. Chim. Acta* **1996**, *251*, 111-118. (c) Cini, R.; Fanizzi, F. P.; Intini, F. P.; Pacifico, C.; Natile, G. Platinum amides from platinum nitriles: X-ray crystal structure of trans-dichloro-bis(1-imino-1-hydroxy-2,2-dimethylpropane)platinum(II). *Inorg. Chim. Acta* **1997**, *264*, 279-286. (d) Cini, R.; Intini, F. P.; Maresca, L.; Pacifico, C.; Natile, G. Isomerism of Amides Coordinated to Platinum – X-ray Crystal Structure of O-Bonded Acetamide in a Platinum(II) Complex. *Eur. J. Inorg. Chem.* **1998**, *1998*, 1305-1312. (e) Cini, R.; Fanizzi, F. P.; Intini, F. P.; Maresca, L.; Natile, G. Platinum amides from platinum nitriles: x-ray crystal structures of the unbridged dinuclear compounds bis[bis(1-imino-1-hydroxy-2,2-dimethylpropane)dichloroplatinum(II)] and bis[bis(1-imino-1-hydroxy-2,2-dimethylpropane)(1-amino-1-oxo-2,2-dimethylpropane)dichloroplatinum(II)]. *J. Am. Chem. Soc.* **1993**, *115*, 5123-5131. (f) Woon, T. C.; Fairlie, D. P. Amide complexes of (diethylenetriamine)platinum(II). *Inorg. Chem.* **1992**, *31*, 4069-4074. (g) Fairlie, D. P.; Woon, T. C.; Wickramasinghe, W. A.; Willis, A. C. Amide-Iminol Tautomerism: Effect of Metalation. *Inorg. Chem.* **1994**, *33*, 6425-6428.
25. (a) For a related chelate formed by two P-OH groups and triflate, see: Wang, X.-B.; Goto, M.; Han, L.-B. Efficient Asymmetric Hydrogenation of α-Acetamidocinnamates through a Simple, Readily Available Monodentate Chiral H-Phosphinate. *Chem. Eur. J.* **2014**, *20*, 3631-3635. (b) With similar cationic Pt precursors (ref 11), both triflate and other weakly coordinating anions yielded active catalysts.
26. (a) Lowe, G.; Sproat, B. S. ^{18}O-isotope shifts on the ^{31}P nuclear magnetic resonance of adenosine-5′-phosphate and inorganic phosphate. *J. Chem. Soc., Chem. Commun.* **1978**, 565-566. (b) Cohn, M.; Hu, A. Isotopic ^{18}O shift in ^{31}P nuclear magnetic resonance applied to a study of enzyme-catalyzed phosphate—phosphate exchange and phosphate (oxygen)—water exchange reactions. *Proc. Natl. Acad. Sci. U. S. A.* **1978**, *75*, 200-203. (c) Lowe, G.; Potter, B. V. L.; Sproat, B. S.; Hull, W. E. The effect of ^{17}O and the magnitude of the ^{18}O-isotope shift in ^{31}P nuclear magnetic resonance spectroscopy. *J. Chem. Soc., Chem. Commun.* **1979**, 733-735.
27. (a) Jensen, C. M.; Trogler, W. C. Kinetics and mechanism of nitrile hydration catalyzed by unhindered hydridobis(phosphine) platinum(II) complexes. Regioselective hydration of acrylonitrile. *J. Am. Chem. Soc.* **1986**, *108*, 723-729. (b) Tamura, M.; Satsuma, A.; Shimizu, K.-i. CeO_2-catalyzed nitrile hydration to amide: reaction mechanism and active sites. *Catal. Sci. Technol.* **2013**, *3*, 1386-1393. (c) Singh, K.; Sarbajna, A.; Dutta, I.; Pandey, P.; Bera, J. K. Hemilability-Driven Water Activation: A Ni^{II} Catalyst for Base-Free Hydration of Nitriles to Amides. *Chem. Eur. J.* **2017**, *23*, 7761-7771. (d) Liu, Y.-M.; He, L.; Wang, M.-M.; Cao, Y.; He, H.-Y.; Fan, K.-N. A General and Efficient Heterogeneous Gold-Catalyzed Hydration of Nitriles in Neat Water under Mild Atmospheric Conditions. *ChemSusChem* **2012**, *5*, 1392-1396. (e) Kumar, D.; Nguyen, T. N.; Grapperhaus, C. A. Kinetic Effects of Sulfur Oxidation on Catalytic Nitrile Hydration: Nitrile Hydratase Insights from Bioinspired Ruthenium(II) Complexes. *Inorg. Chem.* **2014**, *53*, 12372-12377.
28. (a) Glueck, D. S. Asymmetric Synthesis of P-Stereogenic Secondary Phosphine Oxides (SPOs). *Synthesis* **2022**, *54*, 271-280. (b) Zimmerman, A. N.; Xu, R. S.; Reynolds, S. C.; Shipp, C. A.; Marshall, D. J.; Wang, G.; Blank, N. F.; Gibbons, S. K.; Hughes, R. P.; Glueck, D. S.; Balaich, G. J.; Rheingold, A. L. Diastereoselective Synthesis of P-Stereogenic Secondary Phosphine Oxides (SPOs) Bearing a Chiral Substituent by Ring Opening of (+)-Limonene Oxide with Primary Phosphido Nucleophiles. *J. Org. Chem.* **2020**, *85*, 14516–14526.
29. Bandini, A. L.; Banditelli, G.; Cinellu, M. A.; Sanna, G.; Minghetti, G.; Demartin, F.; Manassero, M. Dppf Complexes of Platinum(II) and Platinum(I). Crystal and Molecular Structure of $[dppfPt(\mu\text{-}H)(\mu\text{-}CO)]_2[BF_4]\cdot 0.5H_2O$. *Inorg. Chem.* **1989**, *28*, 404-410.
30. Kendall, A. J.; Seidenkranz, D. T.; Tyler, D. R. Improved Synthetic Route to Heteroleptic Alkylphosphine Oxides. *Organometallics* **2017**, *36*, 2412–2417.